Progress in Oceanography 223 (2024) 103231

Contents lists available at ScienceDirect

Progress in Oceanography

journal homepage: www.elsevier.com/locate/pocean

Consumer isoscapes reveal heterogeneous food webs in deep-sea submarine canyons and adjacent slopes

Amanda W.J. Demopoulos [a,*], Brian J. Smith [b], Jill R. Bourque [a], Jason D. Chaytor [c], Jennifer McClain-Counts [a], Nancy Prouty [d], Steve W. Ross [e], Sandra Brooke [f], Gerard Duineveld [g], Furu Mienis [g]

[a] U.S. Geological Survey (USGS) Wetland and Aquatic Research Center, Gainesville, FL, 32653, United States
[b] Utah State University, Logan, UT 84322, United States
[c] USGS, Woods Hole Coastal and Marine Science Center, Woods Hole, MA 02532, United States
[d] USGS, Pacific Coastal & Marine Science Center, Santa Cruz, CA 95060, United States
[e] University of North Carolina, Wilmington, NC, United States
[f] Florida State University, Coastal and Marine Lab, St. Teresa, FL, United States
[g] NIOZ Royal Netherlands Institute for Sea Research, Den Burg, the Netherlands

ARTICLE INFO

Keywords:
Stable-isotope analysis
Food web
Isoscapes
Deep sea
Slopes
Submarine canyon
U.S. Mid Atlantic

ABSTRACT

The deep sea is the largest biome on earth, but one of the least studied despite its critical role in global carbon cycling and climate buffering. Deep-sea organisms largely rely on particulate organic matter from the surface ocean for energy – these organisms in turn play critical roles in energy transport, transformation, storage, and sequestration of carbon. Within the deep sea, submarine canyons are amongst the most complex and dynamic environments in our oceans, where varied morphology, powerful currents, and variable nutrient conditions influence the distribution of species and transport of organic material throughout the water column and the seafloor. Significant habitat heterogeneity provides ideal substrates for cold-water corals, making submarine canyons of interest to conservation and management. However, how these and other topographic features in the deep ocean influence energy flow and trophic pathways is poorly known. Thus, submarine canyons serve as model systems to track variability in organic material flux and consequential utilization and assimilation by the benthos. In this study, we used an extensive stable isotope dataset to examine food-web structure in Baltimore and Norfolk submarine canyons and compared them to their adjacent slopes located along the U.S. Atlantic margin. Linear models were used to construct geospatially-explicit consumer isoscapes that predicted variation in carbon and nitrogen isotopes across the canyon-slope seascape, providing a predictive map from which to test hypotheses on the distribution and flow of energy resources, relevant to understanding whole community function. Communities were composed of isotopically diverse feeding groups with photosynthetically-derived organic carbon providing the basal food resource. Canyon communities were distinct from the slope, with canyon consumers significantly ^{13}C-depleted, indicating a greater supply and/or utilization of fresh organic matter compared to the slope. Isoscapes for benthic and suspension feeders were distinct, possibly due to the consumption of different quality organic matter sources (fresh = suspension feeders, old = benthic feeders), each with distinct isotope composition. To our knowledge, our modeled isoscapes represent the first spatially extensive isotopic maps of deep-sea consumers, providing insights into regional-scale variation in stable carbon and nitrogen isotopes for different consumer groups. They provide a baseline for tracking climate-change induced fluctuations in the quality and availability of surface primary production and the consequential impact to benthic communities, which play critical roles in carbon cycling in our world's oceans.

* Corresponding author.
E-mail address: ademopoulos@usgs.gov (A.W.J. Demopoulos).

https://doi.org/10.1016/j.pocean.2024.103231
Received 29 March 2023; Received in revised form 11 December 2023; Accepted 26 February 2024
Available online 28 February 2024

1. Introduction

The deep sea encompasses more than half of the earth's surface, representing our planet's largest, and arguably least studied, biome (Ramirez-Llodra et al., 2010). Deep-sea organisms rely on input of particulate organic matter (POM) from the surface ocean as a primary food source, providing a critical function in cycling, remineralization, and sequestration of carbon. This material is transported to the seafloor either directly through deposition or indirectly via diel vertical migrators, including zooplankton, cephalopods, and fishes (Gage and Tyler, 1991; Klages et al., 2003; Inthorn et al., 2006; Trueman et al., 2014). The deep-sea food limitation paradigm posits that POM quantity and availability declines with depth; however, some deep-sea environments experience a decoupling of this food supply/depth paradigm, including areas where organic matter (OM) is produced *in situ* (e.g., chemosynthetic habitats) and/or where highly variable organic-carbon deposition or erosion occurs (e.g., submarine canyons (De Leo et al., 2010)). Climate models predict decreases in particulate organic flux with climate change; this food limitation will in turn impact biodiversity, composition, biomass, and function of deep-sea communities (Jones et al., 2014, Woolley et al., 2016). However, given these changes are predicted to impact a variety of deep-sea environments (Jones et al., 2014), including seamounts and submarine canyons, there is a paucity of understanding how these changes will scale across the local seascape, including geologically complex areas, (e.g., canyon and adjacent slope), and influence the food-web ecology, biodiversity, and ecosystem function.

Much like their terrestrial analogs, submarine canyons exhibit a high degree of topographic complexity, inferred from canyon morphology (e.g., steepness and length), influencing extreme variations in turbulent fluid flow, particle transport and deposition (e.g., Gibbs et al., 2020). Variable flow can influence food quality and supply to consumers within canyons and in adjacent slope environments. Resuspension of fine particulates due to local hydrodynamics, e.g., internal tides, can create nepheloid layers at discrete depths – these layers are concentrated suspended material that includes POM (Kiriakoulakis et al., 2011, Haalboom et al., 2021), serving as a food source for deep-sea fauna (Demopoulos et al., 2017a, b). The channeling and deposition of POM, both functions of canyon morphology and hydrodynamics, increase benthic productivity (Duineveld et al., 2001), faunal abundance and distributions (De Leo et al., 2010, McClain and Barry, 2010, Cunha et al., 2011, Rumolo et al., 2015; Chauvet et al., 2018, Pearman et al., 2020) and trophic complexity (Stefanescu et al., 1994; Cartes and Sorbe, 1999; Cartes et al., 2010; Romero-Romero et al., 2016). Thus, interactive hydrodynamic and geomorphological processes, including resuspension and deposition events controlled by turbidity currents, control food supply to canyon seafloor environments, rather than depth-related food-limitation, which may also influence ecological niche space and biodiversity in submarine canyons (Dell'Anno et al., 2013).

Approximately 6000 submarine canyons occur worldwide (De Leo et al., 2010, Harris and Whiteway, 2011). Stable isotope analysis (SIA) has been used to reveal provenance of POM sources (Prouty et al., 2017, Gibbs et al., 2020), and disentangle complex food webs in submarine canyons and contrast them with other deep-sea environments (Cartes and Sorbe, 1998, Schmiedl et al., 2000, Duineveld et al., 2001, Bianchelli et al., 2008, Cartes et al., 2010, Mamouridis et al., 2011, Fanelli et al., 2013, Papiol et al., 2013, Cartes et al., 2014, Romero-Romero et al., 2016). Recently, detailed examination of Baltimore Canyon and adjacent slope environments (U.S. Atlantic Margin) using stable isotopes and isotopic niche modeling revealed a high degree of trophic complexity across feeding groups within the canyon environments (Demopoulos et al., 2017a, b). Higher trophic diversity and distinct isotopic niches were evident for canyon suspension feeders compared to fauna that consume OM deposited on the seafloor (e.g., benthic feeders, including surface deposit feeders) (Demopoulos et al., 2017a, b). Given a consumer's ecological niche is a function of its abiotic and biotic interactions with its environment (Hutchinson, 1957,1978), heterogeneous environments, like those found in submarine canyons, may be just as important as trophic variability in defining an organism's isotopic niche. Greater sub-habitat heterogeneity leads to greater variation in resource use (Reddin et al., 2018). However, despite the presence of numerous shelf-indenting canyons and extensively canyonized and gullied slopes within the U.S. Atlantic margin (Obelcz et al., 2014), the degree to which this trophic complexity is generalizable to other canyons and over large spatial scales, including along the canyon channels, steep walls, and adjacent slopes, is unknown.

One technique used to estimate variation in isotopic composition over large spatial scales is to create models of isoscapes, which are spatially explicit predictions of isotope values across a landscape (Cheesman and Cernusak, 2016) or "seascape" as in the case of submarine canyons. Isoscapes are created through interpolating geographically dispersed stable isotopic measurements or models that attempt to predict observed heterogeneity from an understanding of isotopic fractionation and associated controls on that fractionation (Cheesman and Cernusak, 2016). These maps can be used to track consumer locations and their geographic origin, and identify dominant carbon and nitrogen sources/dynamics, across geographic and ecological scales (West et al., 2008, Bowen, 2010). This approach enables predictions on a broader scale beyond the confines of the spatial scale sampled, tracing material fluxes from source to sink, monitoring ecosystem-scale processes over time and space (Hellmann and Werner, 2016), and providing insights into community-level interactions (Cheesman and Cernusak, 2016). By coupling isotopic applications with spatial (e.g., GIS techniques) and temporal analyses with other explanatory variables, including seafloor terrain (Wilson et al., 2007, Huvenne et al., 2011), it is possible to infer underlying processes and species interactions, which has been linked to OM flows in the deep sea. However, in the deep sea, understanding of spatially explicit isotopic baselines through isoscapes, and the role that habitat heterogeneity may play in influencing isotopic variation in consumers is unknown.

Marine isoscapes reveal trophic connections and migrations (Navarro et al., 2013; Radabaugh et al., 2013; Trueman et al., 2017; Carpenter-Kling et al., 2020; St John Glew et al., 2019, 2021), however, isoscape modeling approaches have been limited to the open ocean, water column, and/or coastal environments (Thibault et al., 2020, Durante et al., 2021). These isoscapes have examined spatio-temporal changes in isotopic baselines (carbon and nitrogen sources), including primary and secondary production in the surface ocean and water column (McMahon et al., 2013, Navarro et al., 2013, Brault et al., 2018, Waite et al., 2019, Troina et al., 2020, Durante et al., 2021, Ho et al., 2021), revealing major biogeochemical zones on ecosystem-wide scales (Vokhshoori et al., 2014, Carpenter-Kling et al., 2020, Arnoldi et al., 2023), as well as climate-change induced fluctuations in food-web dynamics in the Southern Ocean (St John Glew et al., 2021). The accuracy and applications of isoscapes are limited in areas that are undersampled, reinforcing the value of larger-scale studies that include direct sampling (aka observations) and modeling the relationship between environmental variables. Sessile-dwelling consumer groups, such as suspension-feeding bivalves, can serve as sentinels of change; they integrate and record changes in the isotopic signal of their food, POM (largely phytodetritus) (Jennings and Warr, 2003), over time. Modeled isoscapes of bulk $\delta^{13}C$ values of bivalves reflect the relative distribution of major food sources (Vokhshoori et al., 2014), whereas isoscapes of $\delta^{15}N$ values can reveal variations in nitrogen sources and cycling along spatial gradients. With the inclusion of *in situ* isotope data at local scales, such as those from sessile suspension feeders, regional-scale isoscapes can provide predictions of isotope values in areas where data are lacking or sparse (Trueman and St John Glew, 2019; St John Glew et al., 2021) and ultimately improve applications of isoscapes in marine settings (cf. Bowen et al., 2009, Troina et al., 2020).

In this study, we used SIA from discrete feeding groups found in canyons and adjacent slopes to address the following question: Are

feeding groups found in multiple canyon and adjacent slope environments generally isotopically distinct? We then used linear models to identify key variables that inform isotopic variance, and the top models were used to derive isoscapes for two canyons and adjacent slopes along the U.S. Mid-Atlantic margin. This is the first time, to our knowledge, that isoscapes have been developed for the deep sea. By using seafloor morphology as variables in the models, we linked morphology to isotope patterns in space. Given that habitat heterogeneity and OM supply and quality available to the benthos may differ between canyons and slope environments, we hypothesized that consumer isotopic compositions vary by feeding group, and this variation is location specific over the scales of the canyon and connected slopes. Deep-sea consumer isoscapes have the potential to reveal spatial variability, which may be driven by a number of different factors, including variation in baseline energy sources These baseline isoscapes provide predictive surfaces from which to test ecological questions and discrete hypotheses, including migration patterns for mobile megafauna or distribution of labile carbon down the length of a submarine canyon. Modeled isoscapes presented here may serve as valuable monitoring tools for tracking the impacts of climate change-induced fluctuations in the availability and quality of surface primary production to energy transfer and carbon sources critical to deep-sea consumers.

2. Materials and methods

2.1. Study location

Baltimore and Norfolk canyons are large, shelf-incising canyons within the Mid-Atlantic Basin (Farre et al., 1983). They have distinct differences in overall morphology, differing orientation of the canyon heads, and larger scale hydrodynamics, yet their similarity in depth range, geographic proximity, overall length and size, provide an opportunity for comparisons (Fig. 1). Details on the geomorphology of this region's canyons were documented by Obelcz et al (2014). Both canyons support diverse assemblages of stony and octocorals (Brooke et al., 2017), fishes (Ross et al., 2015), and sediment macrofaunal communities (Robertson et al., 2020). Baltimore Canyon (BC), located 100 km offshore of Maryland, has distinct zones of organic-poor and organic-rich sediments, corresponding to well-defined resuspension (200–600 m, down to 800 m) and deposition regions (>900 m, Gardner, 1989a, b; Mienis et al., 2017). Within the resuspension zone, there is a temporally variable nepheloid layer that extends from 200 to 600 m (sometimes down to 800 m), driven by tidal currents (Gardner, 1989b; Prouty et al., 2017; Ross et al., 2017; Robertson et al., 2020). Current speeds within the deeper reaches of BC approach 9.26 cm s^{-1} at 1082 m and 6.6 cm s^{-1} at 1318 m water depth (Prouty et al., 2017, Robertson et al., 2020). Norfolk Canyon (NC) is located 115 km offshore of Chesapeake Bay. Multiple nepheloid layers are present within NC, where small layers of suspended sediments occur at several depths in the canyon (Ross et al., 2017). In contrast, adjacent slope environments appear free of suspended sediment layers, likely due to the absence of extensive and variable turbidity zones (Gardner, 1989b; Mienis et al., 2017); rather, the slopes experience relatively consistent sediment deposition, characterized by organic content that declines with depth, consistent with other deep-sea environments. Current speeds are notably higher in NC (17.6 cm s^{-1} at 917 m and 9.0 cm s^{-1} at 1364 m) than BC (Ross et al.,

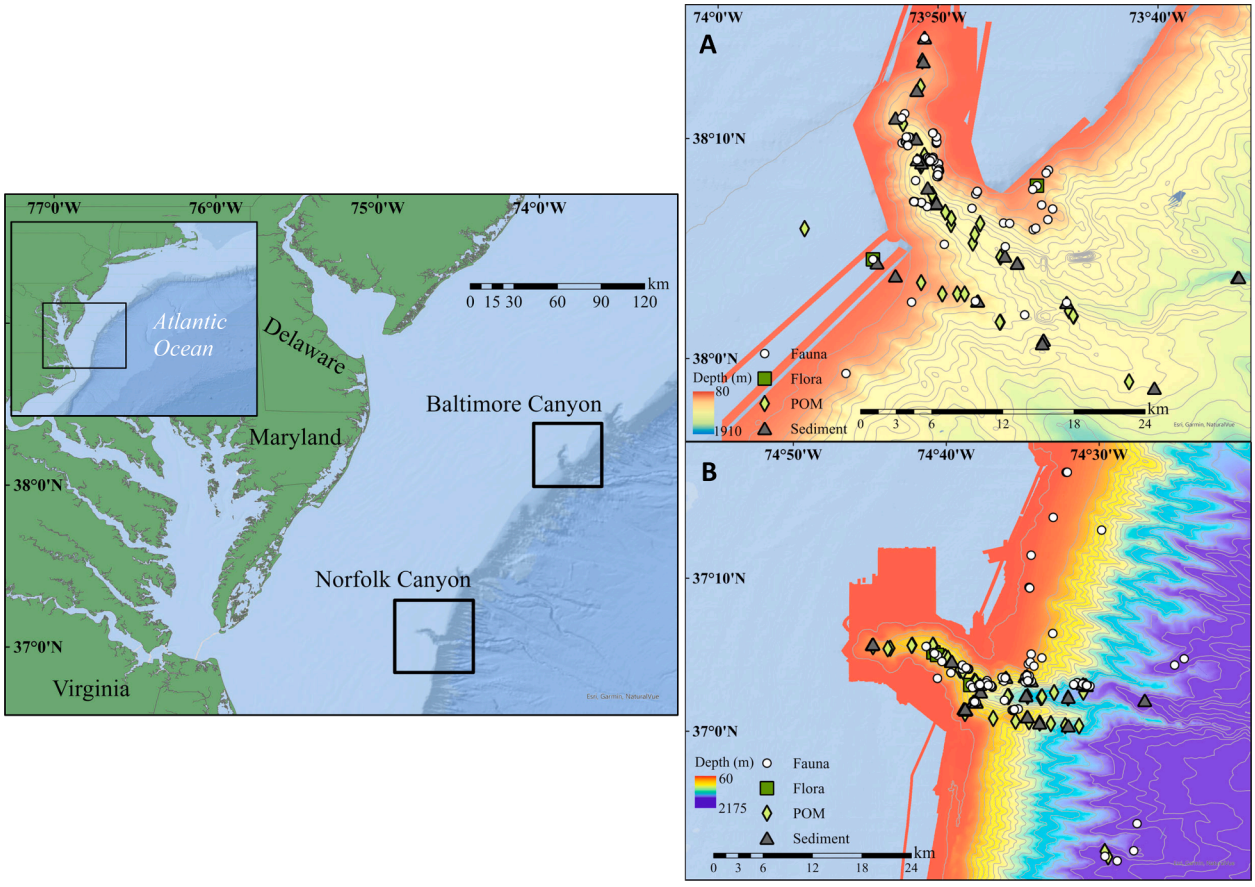

Fig. 1. Location of (A) Baltimore and (B) Norfolk canyons and adjacent slope environments along the U.S. Mid-Atlantic margin. The bathymetry represents 25 m gridded multibeam data with contour lines at every 100 m. Colors on the bathymetric scale represent depth from shallow (red) to deep (blue). Sampling locations from 2011 to 2013 for stable isotope analyses are designated by the following symbols: square = flora, circle = fauna, triangle = sediment, and diamond = particulate organic matter (POM).

2017, Robertson et al., 2020); speeds in both canyons are sufficiently high to facilitate resuspension (or prevent deposition) of material (Gardner 1989b; Thomsen and Gust, 2000).

2.2. Sampling methods

Sampling was conducted within BC and NC and along their respective slopes (Fig. 1) during four research cruises from 2011 to 2013 (Supplementary Table 1). Samples were collected using the NOAA ships *Nancy Foster* (2011, 2012, 2013) and *Ron Brown* (2013) and remotely operated vehicles (ROV) *Kraken II* (2012) and *Jason II* (2013). Multiple gear types, including otter trawls, box cores, ROV push cores, ROV suction sampler, and Niskin bottles were used to sample fauna, POM, and sediments. Otter trawls (4.9 m head rope, 38.1 mm mesh) were deployed and towed for ~ 30 min at ~ 2 knots (3.7 km/h) ground speed to sample benthic fauna. Sediment samples were collected using a Royal Netherlands Institute for Sea Research (NIOZ)-designed box corer with a cylindrical core tube (30 cm diameter, 55 cm height) deployed from the ship. Smaller tube cores (31.65 cm^2 × 30 cm) were inserted into each box core to subsample sediments for analyses. Bottom water was collected with Niskin bottles mounted on a CTD rosette within 10 m of the seafloor and surface seawater was collected within 5–10 m of the surface. Additional water samples were collected at various depths using Niskin bottles attached to the ROVs. Water (up to 10*L*) from each depth was filtered over combusted glass fiber filters. Fauna were collected using either the suction systems or the manipulator arms on the ROVs, while sediments were collected using push cores (31.65 cm^2 × 30 cm) operated by the ROV manipulator arm. Sediment trap samples were collected using two Technicap PPS 4/3 sediment traps mounted on benthic landers with the mouth of traps about 2 m above the bottom and a Honjo Parflux sediment trap mounted on a mooring (4 m above bottom), all programmed to rotate on a 30 day interval at three depths within Baltimore (603 m, 1082 m [mooring], and 1318 m) and Norfolk (630, 917 m [mooring], 1364 m) canyons for the 1-year deployment. Traps were deployed in August and September 2012 (see Supplementary Table 2 for specific dates and locations), and remained in place for up to 1 year. Trap material was preserved in pH buffered solution of mercuric chloride ($HgCl_2$) in seawater to minimize microbial activity and consequential modification of organic matter. Sediment trap samples were divided into five equal splits with a McLane WSD10 rotor splitter at the Royal Netherlands Institute for Sea Research (NIOZ). Two splits were rinsed, frozen, freeze dried, and prepared for isotope analysis (Prouty et al., 2017). Detailed descriptions of the lander and mooring configurations can be found in Ross et al. (2017).

Dissections of fish and invertebrate tissues occurred prior to preservation. For consistency, tissue was removed from similar body regions based on taxa as in Demopoulos et al. (2017a, b). Tissue samples were dried to a constant weight at 50–60 °C, ground to a fine powder and weighed into tin capsules. Invertebrate samples were acidified with 10 % platinum chloride to remove inorganic carbon. POM filters were dried and both filters and sediment trap material were treated with 1.0 N hydrochloric acid, then transferred into tin boats. Surface sediment samples (0–2 cm) were homogenized prior to drying then acidified with 1.0 N phosphoric acid and redried before weighing into tin boats.

Samples (tissue, sediment, POM) were processed as in Demopoulos et al., (2008, 2017a, b) and analyzed for $\delta^{13}C$ and $\delta^{15}N$ values referenced to Vienna PeeDee Belemnite and atmospheric nitrogen gas, respectively. Analyses were conducted at Washington State University using a Costech elemental analyzer interfaced with a GV instruments Isoprime isotope ratio mass spectrometer. Isotope ratios were expressed as $\delta^{13}C$ and $\delta^{15}N$, in per mil (‰). Reported $\delta^{13}C$ values were taken from analyzed acidified samples and $\delta^{15}N$ values from non-acidified samples to avoid the potential artefact associated with acidification (Pinnegar and Polunin, 1999). Precision and accuracy examined through replicate analysis of laboratory standards were less than 0.2‰ in C and N (Demopoulos et al., 2008). Specific laboratory standards used included bovine liver, egg albumin, and acetanilide.

2.3. Data processing

All data presented represent untransformed means (±1 S.E.). Bottom-water POM and sediment stable isotope data were compared using a one-way analysis of variance (ANOVA). All data were tested for normality and heteroscedasticity using Shapiro-Wilk and Levene's tests (Zar, 1999). If data were not normally distributed, then a non-parametric Kruskal-Wallis test was used, followed by post-hoc pairwise Wilcoxon tests. All raw data are available in Demopoulos et al. (2017c), Demopoulos et al. (2024), and McClain-Counts et al. (2018).

Feeding group assignments (benthic [BE], pelagic [PE], suspension [SS], benthic/pelagic [BP], deposit/suspension [DS], and unknown [UK]) and definitions were based on literature review (Supplementary Table 2, Demopoulos et al., 2017a, b). Feeding groups were defined as follows: benthic feeders included deposit, infaunal, epibenthic, and suprabenthic feeders, as well as those identified mixed groups (any combination of deposit, infauna, epibenthic or suprabenthic feeders). These benthic subcategories are further defined in the Supplementary materials. Pelagic feeders were mobile fauna that consumed prey in the water column. Benthic/pelagic feeders fed on taxa associated with the seafloor and the water column. Deposit/suspension feeders rely on material that is floating in suspension and deposited on the seafloor. Suspension feeders are attached to the substrate, consuming organic material that is suspended in the water column. A few taxa were classified as unknown feeding group, due to insufficient taxonomic resolution (e.g., Decapoda-Shrimp).

For trawl samples, we assigned the latitude, longitude, and depth to isotope samples based on the ship's position and water depth at the start of sampling (at the time when the net reached sampling depth). For trawls NF-2012–150 and 168, there was a malfunction with the trawl winch, so the ship's position and the water depth at the location where the net was deployed were used for those stations. For ROV collections, post-processed navigation data including the position and depth of the ROV at the time of sampling were recorded. Lastly, for CTD water samples, the ship's position and depth recorded by the CTD were used. Lander and mooring locations were approximated through triangulation of three points around the location of the lander/mooring.

We considered the 13 variables for inclusion in our models (Table 1) as follows: one categorical variable ("In/Out", where in = within the

Table 1
Candidate terrain variables in the model set of each isotope.

Name	Units	Description
In/Out	Categorical	Whether sample was taken inside or outside the canyon
Depth	Meters	Water depth of sample collection
SD(Depth)	Unitless	Standard deviation of depth within a neighborhood of 3x3 cells
Slope	Degrees	Maximum change in depth in a neighborhood of 3x3 cells
SD(Slope)	Unitless	Standard deviation of slope within a neighborhood of 3x3 cells
tan(Curve)	Unitless	Tangential curvature describes/characterizes divergence or convergence of flow across a surface
BPI broad	Unitless	Broad bathymetric position index – relative vertical position of the sampling location in a radius of 10 cells
BPI fine	Unitless	Fine bathymetric position index - relatively vertical position of the sampling location in a radius of 3 cells
Rugosity	Unitless	Terrain complexity – the ratio of surface area to planar area
cos(Aspect)	Unitless	Cosine of aspect (direction of maximum slope) in radians
cos(2 x Aspect)	Unitless	Cosine of 2 times aspect in radians (double the period of the wave)
sin(Aspect)	Unitless	Sine of aspect in radians
sin(2 x Aspect)	Unitless	Sine of 2 times aspect in radians (double the period of the wave)

canyon, out = adjacent slope), eight continuous variables, and four transformations of a circular variable ("Aspect") as recommended by deBruyn and Meeuwigg. (2001). We removed observations with missing values for any covariate. Lastly, we scaled and centered all eight continuous terrain variables to improve model fitting and parameter interpretation. The seafloor terrain variables (Table 1) were calculated from 10 m and 25 m gridded (cell) resolution multibeam bathymetry surfaces constructed from multiple surveys conducted across the region (Andrews et al., 2016). ArcGIS 3D Analyst and Spatial Analyst Tools were used to calculate depth, standard deviation of the depth, slope, standard deviation of the slope, and aspect of the slope (to derive easting and northing calculated using sine and cosine transformed aspect, respectively). The Benthic Terrain Modeler (BTM) 3.0 toolbox (Walbridge et al., 2018) in ArcMap 10.5 was used to extract additional variables including rugosity (terrain ruggedness), fine-scale bathymetric profile index (BPI) to identify smaller features of the canyon and slope landscape, and a broad-scale BPI to identify larger regions in that landscape. Tangential curvature was calculated using DEM Surface Tools (Jenness, 2013).

Consideration was given regarding the impact of lipids on bulk $\delta^{13}C$ values. Lipids may be ^{13}C-depleted, and it has been suggested that for samples with variable lipid content, a normalization should be applied to the data prior to analysis (Post et al., 2007). Data were examined for potential lipid contribution and for samples that had C:N values > 3.5, their corresponding $\delta^{13}C$ values were mathematically corrected for the effect of lipid concentration on $\delta^{13}C$ measurements using the methods of Post et al. (2007) for invertebrates and Hoffman and Sutton (2010) for fishes, as used in Demopoulos et al. (2017a, b). Following the correction, the $\delta^{13}C$ values were compared using paired t-tests and differences between the pairs were significant for both fishes ($t = –22.934$, $df = 752$, $p < 0.001$, mean difference = -0.496) and invertebrates ($t = -54.777$, $df = 1558$, $p < 0.001$, mean difference = -1.015). The same analysis was conducted by feeding group with the highest difference occurring in suspension feeders (mean difference = -1.17926, $t = -39.403$, $df = 510$, p-value < 0.001), followed by pelagic feeders (mean difference = -0.9419205, $t = -27.685$, $df = 364$, p-value < 0.001), and lastly, benthic feeders (mean difference = -0.6778935, $t = –33.236$, $df = 1285$, p-value < 0.001). Both corrected and uncorrected data were used in the development of the isoscape models described below to enable comparisons across habitats and broader region. We fit our full model to both raw (not lipid corrected) $\delta^{13}C$ and normalized $\delta^{13}C$ data and compared parameter estimates (Fig. S1). After verifying that all terrain effects were similar between the two models, we chose to proceed with the raw isotope data. Details of our lipid normalization can be found in supplemental material. The final dataset consisted of 1917 samples from the two canyons (724 from Baltimore and 1193 from Norfolk). Most of the organisms collected were categorized as benthic feeders (1070), followed by suspension (428), pelagic (342), and finally the two combination feeding categories (Benthic/Pelagic = 69, Deposit/Suspension = 8).

2.4. Model fitting

We built linear models to describe the relationships between our covariates of interest (listed below) and the observed isotope ratios. We fit all models and performed all subsequent analyses in R version 3.6.3 (R Development Core Team, 2020). We built separate model sets for the $\delta^{13}C$ and $\delta^{15}N$ datasets. Each model set began with a fully parameterized model containing all possible covariates. Each full model contained a categorical variable describing the feeding group, the terrain variables (Table 1), and the canyon (Baltimore or Norfolk). Thus, the full model for each set can be described as:

$$\delta^{H}X = \beta_0 + FeedingGroup + TerrainVariables + Canyon + \epsilon$$

$$\epsilon \sim N(0, \sigma^2)$$

where β_0 is the population-level intercept and ϵ represents the residual error term. We assessed goodness-of-fit of the full model with adjusted-R^2.

After fitting the full model for each isotope, we used the function 'dredge()' from the package 'MuMIn' to fit all possible combinations of terrain variables, while keeping feeding group and canyon in every model (Barton, 2018). With 13 possible terrain variables (including the transformations of aspect), the resulting model sets had 2^{13} = 8,192 candidate models per isotope. We ranked the models using AICc (AIC corrected for finite sample size), and then used model averaging to combine the parameter estimates for all competitive models (<2 ΔAICc). For model averaging, we used the function 'model.avg()' in the package 'MuMIn', using the full average, as opposed to the conditional average (i.e., we assumed that each variable had a parameter estimate of 0 if did not appear in a given candidate model). This approach resulted in a single average model for each isotope.

2.5. Isoscape construction

The averaged models were used to predict isotopic variation across both Baltimore and Norfolk canyons and adjacent slopes, thus generating a model-based isoscape of the two canyon areas. We generated isotopic predictions for the primary feeding groups (benthic, pelagic, and suspension), but not for the mixed groups (benthic/pelagic and deposit/suspension) given their small sample sizes. Before generating the isoscapes, we first checked the model residuals for spatial autocorrelation to verify that the model captured the meaningful spatial pattern and that the corresponding residuals were independent. We checked for spatial autocorrelation using non-parametric spline correlograms from the package 'ncf' (Bjørnstad, 2019). Prior to fitting the spatial correlation model, we needed to jitter the locations taken at the same spot by 2–10 m using the function 'jitterDupCoords()' from the package 'geoR' (Ribeiro and Diggle, 2001).

Spatial covariates were available as raster data with two different cell resolutions: 10 m and 25 m. We fit our full model (see "Model Fitting") to data from both scales and compared parameter estimates. After confirming that all parameter estimates were similar (Fig. S2), we chose the finer grain (10 m) for subsequent analyses and reported predictions. Details of our scale comparison are available in the supplemental material. In addition, given the similarities between parameter estimates for lipid corrected and raw $\delta^{13}C$ data (Fig. S1), we chose non-lipid corrected (raw) data for our linear models to limit assumptions. The final dataset consisted of 1917 samples from the two canyons (724 from Baltimore and 1193 from Norfolk). Most of the organisms collected were categorized as benthic feeders (1070), followed by suspension (428), pelagic (342), and finally the two combination feeding categories (Benthic/Pelagic = 69, Deposit/Suspension = 8).

2.6. Model validation using canyon zones

Given the spatial differences in the depositional environments associated within the canyon and adjacent slope (see Materials and methods-2.1 *Study location* above), we hypothesized that this might result in differences in the model predicted isotope values throughout distinct zones of each canyon. This analysis involved a post-hoc examination of the residuals for each feeding group in each zone. The two canyon environments were subdivided into zones characterized as channel, slope, or wall. Channels (Channel Zone) were classified as the flat to low gradient seafloor at the base of the steep gradient canyon walls (Wall Zone). Walls transition to the shelf and continental slope (Slope Zone) along the maximum change in gradient at the top of the canyon walls or canyon bounding ridges (drainage divides). For all samples in the model, we calculated the residual between the observed values and the model-predicted values, and then grouped the residuals by zone and feeding group. This represents an in-sample model

validation, but since the grouping was based on a covariate not used in model building (zone), our goal was to identify any systematic spatial differences in the model's predictive ability.

3. Results

3.1. General patterns

A total of 3032 samples, representing 11 phyla, as well as sediments, POM (from both bottom [POM_b] and surface water [POM_s]), and sediment trap samples, were analyzed for $\delta^{13}C$ and $\delta^{15}N$ (Table 2, Supplementary Tables 3, 4). Stable carbon isotope data for the primary sources analyzed ranged from −24.2 to −12.6 ‰. (Table 2). Stable carbon and nitrogen isotope values for the sediment traps deployed within the canyons ($\delta^{13}C$: –22.8 to –22.0 ‰, $\delta^{15}N$: 4.3 to 5.1 ‰) were within the range of POM (bottom and surface) and sediment isotope values and were very consistent across sampled depths. POM_b from NC was ^{13}C-enriched compared to BC (ANOVA $F_{1,28} = 20.216$, $p < 0.001$), while BC POM was ^{15}N-enriched relative to NC (ANOVA $F_{1,28} = 14.829$, $p < 0.001$). However, there was no significant difference in POM_b isotope values between the slope environments adjacent to BC and NC ($\delta^{13}C$ ANOVA $F_{1,7} = 3.1501$, $p = 0.119$; $\delta^{15}N$ KW $x^2 = 0.242$, $p = 0.623$). Temporal variability in POM could only be tested for POM_s from NC, which was ^{13}C-enriched in May 2013 (-21.1 ‰), compared to November 2012/2013 (–23.5 to –23.1 ‰, One-way ANOVA: $F_{2,23} = 4.918$, $p < 0.05$). Sediment $\delta^{13}C$ values did not differ between BC and NC (ANOVA $F_{1,51} = 3.213$, $p = 0.079$), while NC sediments were slightly ^{15}N-enriched (KW $x^2 = 5.258$, $p < 0.05$) relative to BC. Sediment isotopes did not differ between Baltimore and Norfolk slope habitats (BS and NS, respectively) for either $\delta^{13}C$ (ANOVA $F_{1,27} = 2.158$, $p = 0.153$) or $\delta^{15}N$ (KW $x^2 = 0.584$, $p = 0.444$).

Across the region (combining Norfolk and Baltimore data), POM_b was ^{15}N-enriched compared to POM_s for both canyon and slope environments. While there were no significant differences between canyon and slope $\delta^{13}C$ values for POM_b (KW, $x^2 = 2.156$, $p = 0.142$) or sediment (ANOVA: $F_{1,80} = 0.0737$, $p = 0.787$), canyon POM_b and sediments were ^{15}N-enriched relative to slope habitats ($\delta^{15}N$, POM_b: ANOVA, $F_{1,37} = 4.523$, $p < 0.05$; sediment: KW, $x^2 = 5.089$, $p < 0.05$). Canyon sediments were significantly ^{13}C-enriched relative to canyon POM_b ($\delta^{13}C$: KW, $x^2 = 11.547$, $p < 0.001$). Likewise, slope sediments were ^{13}C-enriched relative to slope POM_b (ANOVA, $F_{1,36} = 13.191$, $p < 0.001$). However, there was no difference in $\delta^{15}N$ between these two primary sources (POM and sediments) for either canyon (ANOVA, $F_{1,81} = 0.458$, $p = 0.5005$) or slope (ANOVA, $F_{1,36} = 0.0787$; $p = 0.7807$) environments. Canyon sediments were both ^{13}C- and ^{15}N-enriched compared to sediment trap samples ($\delta^{13}C$: KW, $x^2 = 18.432$, $p < 0.001$; $\delta^{15}N$: KW, $x^2 =$

Table 2
Stable isotope values ($\delta^{13}C$, $\delta^{15}N$) and C:N ratio for primary producers and sediments collected from Baltimore and Norfolk Canyons, and the adjacent slopes. Values represent the average (±S.E.) with ranges (min to max). Bottom POM was collected within 10 m of the seafloor, while surface POM was collected within 5 m of the surface. Surface sediments were analyzed from the upper 0–2 cm fraction of a push core. Data from sediment trap (Trap) samples were previously published in Mienis et al., 2017.

		Baltimore Canyon (BC)			Baltimore adjacent slope (BS)			Norfolk Canyon (NC)			Norfolk adjacent slope (NS)		
	TaxaID	n	Mean ± SE	(Min - Max)	n	Mean ± SE	(Min - Max)	n	Mean ± SE	(Min - Max)	n	Mean ± SE	(Min - Max)
$\delta^{13}C$ (‰)	**Phaeophyta**												
	cf. Fucus sp.				4	−18.4 ± 0.2	(-18.9 to −17.8)						
	Sargassum sp.				5	−18.3 ± 0.7	(-20.9 to −17.1)	3	−18.3 ± 1.2	(-20.2 to −16.0)			
	POM												
	bottom	13	–23.2 ± 0.3	(-25.4 to –22.1)	4	–23.3 ± 0.4	(–23.8 to –22.2)	17	−21.8 ± 0.1	(–23.2 to −20.9)	5	−22.4 ± 0.3	(–23.4 to −21.5)
	midwater	5	–22.1 ± 0.5	(–23.6 to −20.4)	2	–22.5 ± 0.3	(–22.8 to –22.2)	12	−21.0 ± 0.5	(–23.3 to −18.8)			
	surface	5	−21.2 ± 0.5	(–22.2 to −20.0)	3	–22.7 ± 0.8	(–23.4 to −21.2)	26	−21.8 ± 0.4	(-24.8 to −18.7)	7	−20.1 ± 0.4	(–22.7 to −19.4)
	Sediment												
	Surface	21	−21.9 ± 0.2	(-24.4 to −19.7)	18	−21.8 ± 0.2	(–22.9 to −20.3)	32	−21.5 ± 0.1	(–23.2 to −20.3)	11	−21.3 ± 0.3	(–23.4 to −19.2)
	Trap	14	–22.3 ± 0.1	(–22.8 to –22.0)				3	–22.2 ± 0.1	(–22.3 to –22.1)			
$\delta^{15}N$ (‰)	**Phaeophyta**												
	cf. Fucus sp.				4	3.3 ± 0.3	(2.6 to 4.0)						
	Sargassum sp.				5	0.9 ± 0.9	(-1.2 to 4.0)	3	1.2 ± 0.6	(0.1 to 1.9)			
	POM												
	bottom	13	7.4 ± 0.5	(3.1 to 9.5)	4	5.9 ± 1.0	(4.0 to 8.2)	17	5.5 ± 0.2	(3.5 to 6.8)	5	4.3 ± 0.6	(2.0 to 5.0)
	midwater	5	5.8 ± 0.8	(4.5 to 8.5)	2	4.4 ± 0.3	(4.1 to 4.7)	12	4.0 ± 0.4	(2.6 to 5.8)			
	surface	5	5.5 ± 1.0	(3.1 to 8.3)	3	3.2 ± 0.7	(2.4 to 4.6)	26	4.6 ± 0.2	(2.2 to 7.4)	7	3.8 ± 0.4	(2.3 to 5.6)
	Sediment												
	Surface	21	5.5 ± 0.4	(1.8 to 8.7)	18	4.5 ± 0.7	(-3.7 to 10.0)	32	6.5 ± 0.3	(1.5 to 10.4)	11	5.1 ± 0.7	(1.1 to 7.5)
	Trap	14	4.8 ± 0.1	(4.3 to 5.0)				3	5.0 ± 0.1	(4.9 to 5.1)			
C:N	**Phaeophyta**												
	cf. Fucus sp.				4	26.7 ± 1.9	(21.3 to 30.3)						
	Sargassum sp.				5	24.9 ± 2.7	(15.8 to 31.3)	3	24.2 ± 7.0	(10.1 to 31.5)			
	POM												
	bottom	13	9.3 ± 0.4	(7.6 to 12.5)	4	8.0 ± 0.8	(6.3 to 9.4)	17	8.4 ± 0.4	(5.3 to 10.7)	5	8.8 ± 0.5	(7.3 to 10.0)
	midwater	5	7.6 ± 0.9	(6.0 to 11.1)	2	6.9 ± 0.2	(6.7 to 7.1)	12	5.6 ± 0.3	(4.4 to 7.8)			
	surface	5	8.3 ± 1.1	(6.7 to 12.6)	3	8.2 ± 0.5	(7.3 to 8.9)	26	8.1 ± 0.3	(5.6 to 11.3)	7	9.9 ± 0.3	(8.4 to 10.5)
	Sediment			8.0 ± 0.9			13.3 ± 2.7			11.3 ± 2.3			5.9 ± 0.9
	Surface	21	8.0 ± 0.9	(2.9 to 19.1)	18	13.3 ± 2.7	(1.2 to 43.6)	32	11.3 ± 2.3	(2.0 to 79.1)	11	5.9 ± 0.9	(0.3 to 9.0)
	Trap	14	9.6 ± 0.2	(8.8 to 10.6)				3	9.3 ± 0.2	(9.1 to 9.7)			

18.354, $p < 0.001$). There was no significant difference between sediment trap and POM_b $\delta^{13}C$ values (KW, $x^2 = 0.126$, $p = 0.722$), but POM_b was ^{15}N-enriched compared to the sediment trap (KW, $x^2 = 13.998$, $p < 0.001$).

Isotope results from feeding groups in canyons and slopes revealed some overlap as well as key differences between these two environments. Stable isotope results revealed that the canyon and slope communities were composed of several feeding groups (Fig. 2, Supplementary Tables 3, 4). Canyon consumers were generally ^{13}C and ^{15}N-depleted relative to consumers on the adjacent slopes (Fig. 2, see centroid means), with suspension feeders having the lowest values, pelagic consumers with intermediate values, and benthic feeders generally having the highest isotope values.

Suspension feeders from BC and BS exhibited a large range in $\delta^{15}N$ values (1.7 to 10.7 ‰), while the range in $\delta^{13}C$ values (-24.3 to −16.6 ‰) was consistent with the range in POM $\delta^{13}C$. The $\delta^{13}C$ values of specific suspension-feeding corals ranged from –22.6 ‰ ± 0.2 SE (*Desmophyllum dianthus* from BC) to −18.6 ‰ ± 0.4 SE (*Dasmosmilia lymani,* from BS), and $\delta^{15}N$ values from 2.7 ‰ ± 0.9 (Alcyonacea sp. 1 from BC) to 7.3 ‰ (n = 1, Alcyonacea sp. 2 from BC). While the range in $\delta^{13}C$ values from NC and NS (-24.4 to −14.5 ‰) was similar to Baltimore, suspension feeders exhibited an even larger range in $\delta^{15}N$ values (-0.1 to 13.9 ‰). Average $\delta^{13}C$ values of suspension-feeding corals ranged from –22.8 ‰ ± 0.4 (Pennatulacea from NC) to −16.6 ‰ (n = 1, Isididae from NS), and $\delta^{15}N$ values from 2.5 ‰ ± 0.4 (*D. lymani* from NS) to 10.4 ‰ ± 0.8 (*Sibopathes* sp. from NC).

Benthic consumers encompassed several “sub” groups, including infaunal, epifaunal, deposit, and suprabenthic feeders. Consumers classified simply as “Benthic” were unable to be further differentiated. Within BC and BS, benthic consumer $\delta^{13}C$ values ranged from –22.2 (n = 1, Annelida from BS) to −13.2 ‰ (n = 1, poranid seastars in BC) and $\delta^{15}N$ values ranged from 5.3 ‰ ± 1.8 (*Colus stimpsoni* from BC) and 5.3 ‰ ± 0.2 (*Paguristes lymani* from BS) to 14.1 ‰ (Asteroida from BC). In NC and NS, benthic consumers had a large range in $\delta^{13}C$ values and similar range in $\delta^{15}N$ values compared to Baltimore region, with $\delta^{13}C$ values ranging from −24.2 (Solenogastres from NC) to −14.4 ‰ ± 0.3 (*Plutonaster agassizi agassizi* from NS) and $\delta^{15}N$ values ranged from 0.6 (*Cidaris* sp. from NS) to 15.1 ‰ (*Malletia* sp. from NS).

Pelagic feeders exhibited a smaller range in $\delta^{13}C$ values compared to benthic and suspension feeders around both Baltimore (-21.3 to −16.2 ‰) and Norfolk (–22.4 to −15.7 ‰) canyons. The squid, *Illex* cf. *illecebrosus* had the lowest $\delta^{13}C$ (-21.3 ‰, n = 1) value and euphausid, *Meganyctiphanes norvegica,* had the lowest $\delta^{15}N$ (6.9 ‰ ± 0.4) values, both were from BC. While the fish, *Argentina striata*, from BS had the highest $\delta^{13}C$ and $\delta^{15}N$ values (-16.8 and 12.4 ‰, respectively, n = 1). In Norfolk, pelagic feeding pyrosomes from NS had the lowest $\delta^{13}C$ (-21.7 ‰ ± 0.4) and $\delta^{15}N$ values (3.0 ± 0.7), whereas *Processa profunda* had the highest $\delta^{13}C$ (-16.6 ‰ ± 0.1), and *Maurolicus weitzmani* had the highest $\delta^{15}N$ (12.7 ‰) values, both from NS.

3.2. Carbon isotope model set

The full model for the carbon model set had an adjusted $R^2 = 0.49$. The model set for $\delta^{13}C$ had 18 models within < 2 ΔAICc from the top model (Table 3). The averaged model for the carbon isotope model set indicated that $\delta^{13}C$ values from Baltimore organisms were on average slightly (0.1 ‰) greater than those from Norfolk. Feeding groups differed in $\delta^{13}C$ by up to 2.3 ‰, with suspension feeders having the lowest $\delta^{13}C$ values and benthic and benthic/pelagic feeders having the highest $\delta^{13}C$ values (Fig. 3). The most important variables identified were “In/Out” (18 models), “Depth” (18 models), “cos(Aspect)” (18 models), “sin(Aspect)” (18 models), “sin(2 x Aspect)” (18 models),

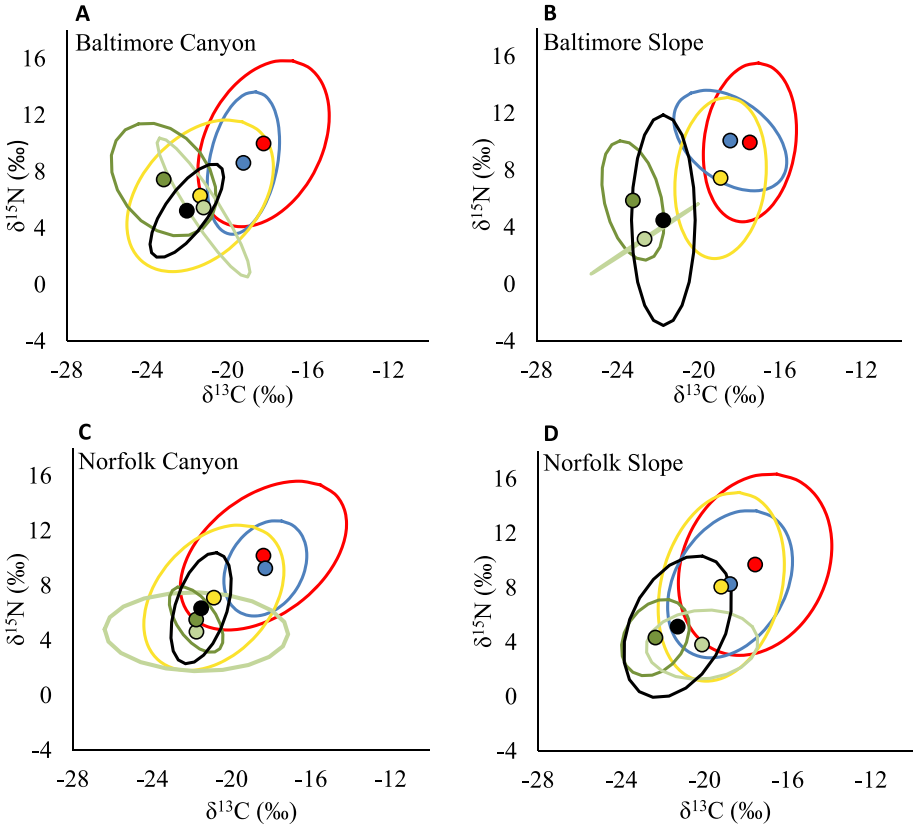

Fig. 2. Isotope data for benthic (red), pelagic (blue) and suspension (yellow) feeders, sediment (black) and bottom (dark green) and surface (light green) POM collected in (A) Baltimore Canyon, (B) Baltimore adjacent slope, (C) Norfolk Canyon and (D) Norfolk adjacent slope. Points represent the mean $\delta^{13}C$ and $\delta^{15}N$ data, and ellipses were created using 95% confidence intervals.

Table 3
Carbon models with 2 ΔAICc of the top model, showing the terrain variables included in the model, the number of parameters in the model, the AICc score, the difference in AICc from the top model (ΔAICc), and the AICc weight (ω).

Model	Parameters	AICc	ΔAICc	ω
In/Out + Depth + cos(Aspect) + sin (Aspect) + sin(2 x Aspect) + Slope + SD(Slope) + SD(Depth) + tan (Curve) + BPI Fine	17	6486.32	0.00	0.04
In/Out + Depth + cos(Aspect) + sin (Aspect) + sin(2 x Aspect) + Slope + SD(Slope) + SD(Depth) + tan (Curve)	16	6486.65	0.33	0.03
In/Out + Depth + cos(Aspect) + sin (Aspect) + sin(2 x Aspect) + Slope + SD(Slope) + SD(Depth)	15	6486.68	0.36	0.03
In/Out + Depth + cos(Aspect) + sin (Aspect) + sin(2 x Aspect) + Slope + SD(Slope)	14	6487.25	0.93	0.03
In/Out + Depth + cos(Aspect) + sin (Aspect) + sin(2 x Aspect) + Slope + SD(Slope) + SD(Depth) + tan (Curve) + BPI Broad	17	6487.81	1.49	0.02
In/Out + Depth + cos(Aspect) + cos(2 x Aspect) + sin(Aspect) + sin(2 x Aspect) + Slope + SD(Slope) + SD (Depth) + tan(Curve) + BPI Fine	18	6487.95	1.63	0.02
In/Out + Depth + cos(Aspect) + sin (Aspect) + sin(2 x Aspect) + Slope + SD(Slope) + SD(Depth) + tan (Curve) + Rugosity + BPI Fine	18	6488.07	1.76	0.02
In/Out + Depth + sin(Aspect) + sin(2 x Aspect) + Slope + SD(Slope) + SD (Depth) + tan(Curve) + BPI Fine	16	6488.17	1.85	0.02
In/Out + Depth + cos(Aspect) + cos(2 x Aspect) + sin(Aspect) + sin(2 x Aspect) + Slope + SD(Slope) + SD (Depth) + tan(Curve)	17	6488.26	1.94	0.02
In/Out + Depth + cos(Aspect) + sin (Aspect) + sin(2 x Aspect) + Slope + SD(Slope) + tan(Curve)	15	6488.26	1.94	0.02

"Slope" (18 models), "SD(Slope)" (16 models), and "SD(Depth)" (14 models). After plotting each of these variables against predicted $\delta^{13}C$, while holding all other terrain variables constant at their mean (Fig. 4), some patterns were evident. Modeled $\delta^{13}C$ values increased with location (Out > In), increased depth, decreased slope and slope variation (SD (Slope)), and $\delta^{13}C$ varied with aspect, indicating that the direction of the slope, whether northwest or southeast facing, influenced $\delta^{13}C$ variability.

3.3. Nitrogen isotope model set

The full model for the nitrogen model set had adjusted $R^2 = 0.36$. The model set for $\delta^{15}N$ had 11 models within < 2 ΔAICc from the top model (Table 4). The averaged model for the nitrogen isotope model set indicated that $\delta^{15}N$ values from Baltimore organisms were on average 0.6 ‰ greater than those from Norfolk. Feeding groups differed in $\delta^{15}N$ by up to 5.4 ‰, with suspension and deposit/suspension feeders having the lowest $\delta^{15}N$ values and benthic feeders having the highest $\delta^{15}N$ values (Fig. 3). The most important terrain variables were "In/Out" (11 models), "Depth" (11 models), "Slope" (11 models), "SD(Slope)" (11 models), and "SD(Depth)" (11 models). Two transformations of aspect appeared in most of the top 11 models: "sin(2 x Aspect)" (11 models) and "sin(Aspect)" (9 models). After plotting each of these variables against predicted $\delta^{15}N$, while holding all other terrain variables constant at their mean (Fig. 5), some patterns were apparent. Predicted $\delta^{15}N$ values increased with increased depth and variability in depth, decreased slope and slope variation (SD (Slope)), and $\delta^{15}N$ varied with aspect, indicating that the direction of the slope, whether northwest or southeast facing, influenced $\delta^{15}N$ variability.

3.4. Spatial prediction

The raw isotopic values in the dataset showed spatial autocorrelation within 1500 m; however, the residuals of the averaged models did not show any strong spatial autocorrelation (Fig. S3). Given this lack of autocorrelation, we created isoscapes for each of the three primary feeding groups (Suspension, Benthic, and Pelagic) for each canyon environment (canyon and surrounding slope) for $\delta^{13}C$ (Fig. 6) and $\delta^{15}N$ (Fig. 7). Parameter uncertainty around each estimate was low; 95 % of the $\delta^{13}C$ estimates had standard errors < 0.19 ‰ and for $\delta^{15}N$, <0.28 ‰. Very few pixels had extreme values (Figs. S4 & S5). For both isotopes, lower values were generally constrained to the steep canyon walls, whereas higher isotopic values were associated with the canyon channel, or thalweg, and the adjacent slope. Pelagic-feeder isoscapes were intermediate between suspension feeders (low range) and benthic feeders (high range).

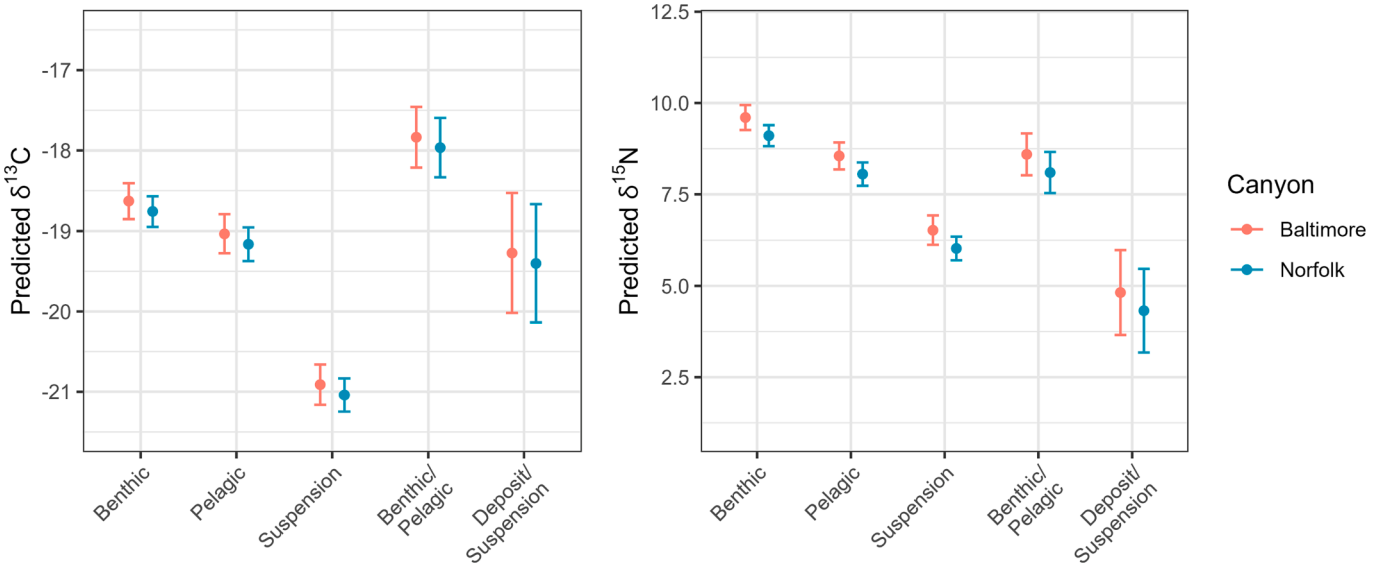

Fig. 3. Predicted mean $\delta^{13}C$ (left) and $\delta^{15}N$ (right) values (‰) for each feeding group from the averaged carbon and nitrogen models. Error bars show 95% confidence intervals around the prediction.

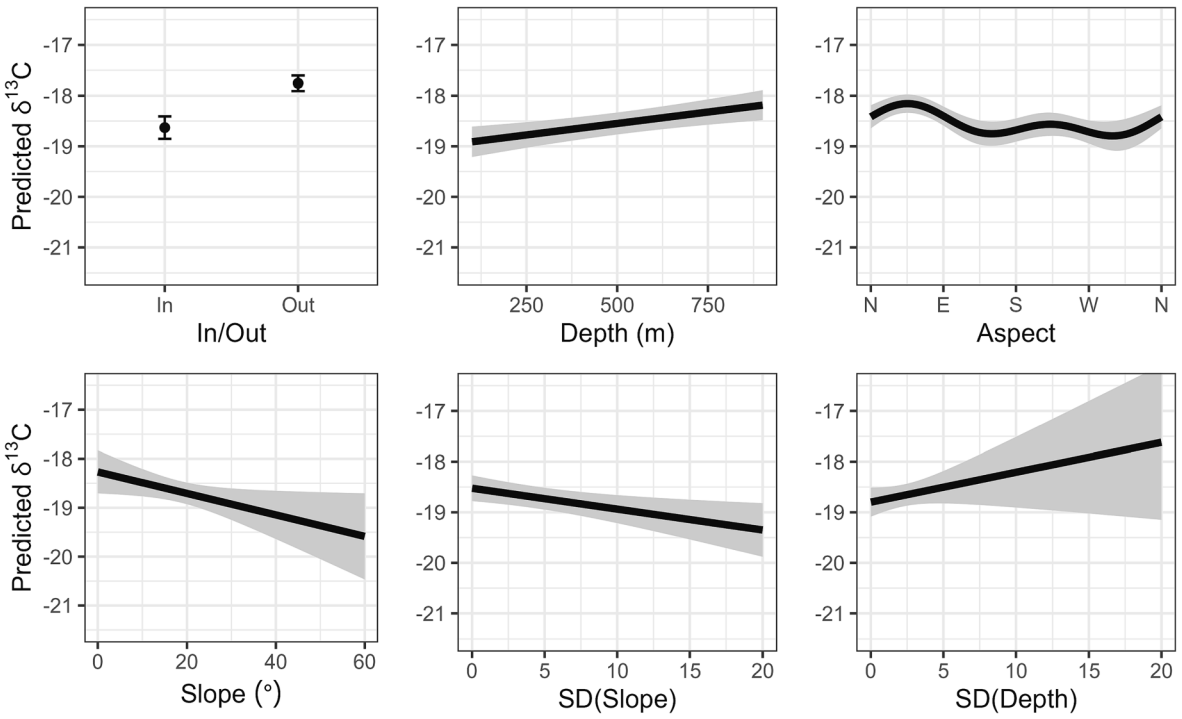

Fig. 4. Predicted mean relationship for the Benthic feeding group between $\delta^{13}C$ values (‰) for each terrain variable that appears in the averaged carbon model. For each prediction, all other continuous variables were held at their mean, the "In/Out" categorical variable was set to "In". Gray envelopes show 95% confidence intervals around the prediction.

Table 4
Nitrogen models within 2 ΔAICc of the top model, showing the terrain variables included in the model, the number of parameters in the model, the AICc score, the difference in AICc from the top model (ΔAICc), and the AICc weight (ω).

Model	Parameters	AICc	ΔAICc	ω
In/Out + Depth + sin(Aspect) + sin(2 x Aspect) + Slope + SD(Slope) + SD (Depth)	14	8201.33	0.00	0.03
In/Out + Depth + cos(Aspect) + sin (Aspect) + sin(2 x Aspect) + Slope + SD(Slope) + SD(Depth)	15	8201.98	0.65	0.02
In/Out + Depth + sin(Aspect) + sin(2 x Aspect) + Slope + SD(Slope) + SD (Depth) + tan(Curve)	15	8202.22	0.89	0.02
In/Out + Depth + cos(2 x Aspect) + sin(Aspect) + sin(2 x Aspect) + Slope + SD(Slope) + SD(Depth)	15	8202.51	1.18	0.02
In/Out + Depth + cos(Aspect) + sin(2 x Aspect) + Slope + SD(Slope) + SD (Depth)	14	8202.62	1.29	0.02
In/Out + Depth + sin(2 x Aspect) + Slope + SD(Slope) + SD(Depth)	13	8202.82	1.49	0.01
In/Out + Depth + cos(Aspect) + sin (Aspect) + sin(2 x Aspect) + Slope + SD(Slope) + SD(Depth) + tan (Curve)	16	8202.90	1.57	0.01
In/Out + Depth + sin(Aspect) + sin(2 x Aspect) + Slope + SD(Slope) + SD (Depth) + Rugosity	15	8203.18	1.85	0.01
In/Out + Depth + cos(2 x Aspect) + sin(Aspect) + sin(2 x Aspect) + Slope + SD(Slope) + SD(Depth) + tan(Curve)	16	8203.21	1.89	0.01
In/Out + Depth + sin(Aspect) + sin(2 x Aspect) + Slope + SD(Slope) + SD (Depth) + BPI Broad	15	8203.32	1.99	0.01

3.5. Model performance in discrete canyon zones (Wall, Channel, Slope)

The canyon zone validation (wall, channel, slope) indicates that the model performed well at predicting isotopic ratios throughout the canyon, with one exception. Predicting the isotopic values of suspension feeders in the canyon channels was consistently challenging, with the mean $\delta^{13}C$ and $\delta^{15}N$ residuals for suspension feeders in the channel was 1.9 ‰ and 2.5 ‰, respectively, while all other residuals were close to 0 (Fig. S6).

4. Discussion

4.1. General patterns

We generated modeled isoscapes for Baltimore and Norfolk submarine canyons and their adjacent slope environments based on > 1900 samples of invertebrates and fishes, illustrating isotopic heterogeneity within and among feeding groups. Spatial variation of faunal isotopes can be due to several factors, including different isotopic baselines in the local food webs, as well as differences in trophic transfer and energy dynamics, and these factors are further discussed below. Ultimately, the geochemical perspective generated from modeling of ecosystem ^{13}C and $\delta^{15}N$ values, as demonstrated for these canyon and slope environments, helps to clarify spatial variability of carbon (cf., Bowen, 2010, Ohshimo et al., 2019) and nitrogen isotope ratios, providing opportunities to test hypotheses regarding food availability and resource use across these areas.

Currently published marine isoscapes from offshore environments are limited to modeling the pelagic food web in the upper water column using POM, phytoplankton, zooplankton, and higher-order pelagic consumers (Navarro et al., 2013, Lorrain et al., 2015, Magozzi et al., 2017, Brault et al., 2018, Arnoldi et al., 2023), as well as sediment isoscapes tracking OM deposition in the Gulf of Mexico (Bosman et al., 2020). In contrast, by developing isoscapes from forage species, e.g., deep-sea suspension feeders examined in this study that integrate

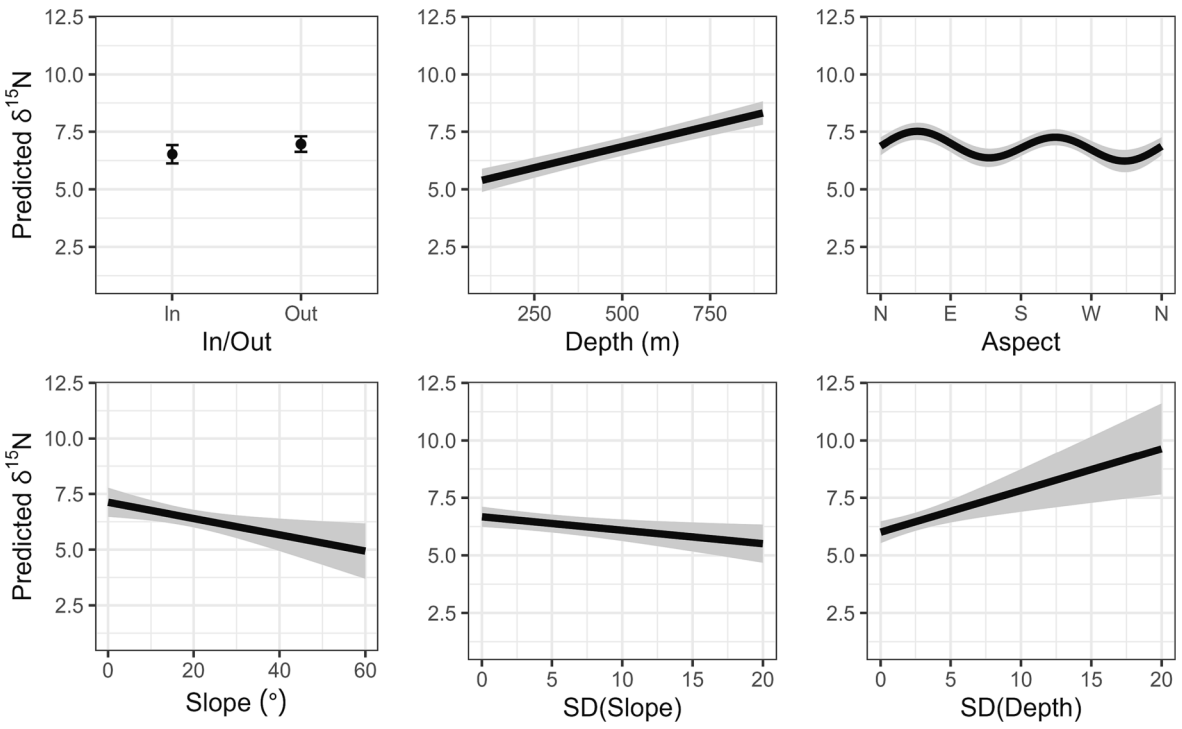

Fig. 5. Predicted mean relationship for the Benthic feeding group between $\delta^{15}N$ values (‰) for each terrain variable that appears in the averaged nitrogen model. For each prediction, all other continuous variables were held at their mean. Gray envelopes show 95% confidence intervals around the prediction.

isotopic variability in local baselines over time in their tissues, we captured local $\delta^{13}C$ and $\delta^{15}N$ dynamics that are less sensitive to irregular fluctuations (Ohshimo et al., 2019).

The high-resolution isoscapes developed for these two canyon and adjacent slope environments were structured by specific variables, including location (in [canyon] vs. out [adjacent slope]), depth, as well as several terrain variables (slope degree, slope variability, and aspect [slope direction]). The resulting isoscapes illustrate key patterns, including low values associated with shallow depths and steep slopes of the canyons, and high values associated with the more gradually sloping environments and deeper areas. Depth is a parameter that co-varies with many other variables, including temperature, dissolved oxygen, and salinity, providing insight into large scale processes, such as water masses. While food availability also generally declines with depth in deep-sea systems, it is often decoupled within the high depositional canyon environments (Duineveld et al., 2001, De Leo et al., 2010, Gibbs et al., 2020, Pearman et al., 2020) such as BC and NC. Slope can serve as a rough proxy for substrate type, where steep slopes often correlate with hard substrates and erosional processes (Pearman et al., 2020); steep slopes are also positively correlated with high diversity of sessile epibenthos, given hard substrates provide suitable attachment sites for epifauna (Baker et al., 2012). The habitat suitability of steep slopes also relates to the controls on sediment deposition, where high slopes can limit deposition of sediment and accelerate erosion, which would otherwise have adverse impacts on sessile fauna, including smothering of tissues and feeding appendages. Lastly, aspect, or slope direction, provides an indication of areas with more or less current exposure (Wilson et al., 2007, Robert et al., 2015, Lo Iacono et al., 2018), which has an influence on sedimentation, food delivery, as well as larval transport. However, whether the isotope variability documented in the current study can be extrapolated to the larger Atlantic margin where dozens of canyons with different morphologies, sediment sources, and oceanographic regimes are present, remains to be evaluated.

4.2. Isoscapes by feeding groups

Overall patterns in the $\delta^{13}C$ and $\delta^{15}N$ data indicate that the canyon and slope food webs are complex, with the large spread in $\delta^{13}C$ indicating a continuum of feeding types from low $\delta^{13}C$ (suspension and pelagic feeders) to high $\delta^{13}C$ (benthic feeders) values (Sherwood et al., 2008), consistent with previous work examining Baltimore Canyon and slope food webs (Demopoulos et al., 2017a). The modeled isoscapes reflected this continuum, where suspension feeders and benthic feeders serve as the low and high isotopic endmembers, with pelagic feeders falling between the two. By modeling the isoscapes based on feeding groups, we capture the range encompassed within each group; focusing on functional grouping rather than species groups circumvents the challenge of not having species evenly distributed across sites and depths. The distinct isoscapes among feeding groups may be a consequence of spatial and temporal isotopic variability in the POM source, including relative contribution of terrestrial vs. marine organic matter (Mienis et al., 2017, Prouty et al., 2017), and/or habitat association. Modeled isoscapes of surface POM within the Atlantic (Magozzi et al., 2017) indicate a relatively constrained range in $\delta^{13}C$ (-20.5 to −19.5 ‰). However, the low resolution of the surface POM isoscapes presented in Magozzi et al. (2017) may not capture regional or local variability present within the Baltimore and Norfolk canyon region, and they do not approximate the isotopic variability of available carbon at depth. Our isoscapes help to fill in that gap and illustrate distinct isotopic gradients that may reflect isotopic variability of POM in space and/or resource use variability among feeding groups.

The isotopic range observed in suspension feeders may reflect differential utilization of both POM and invertebrate prey resources. Some of this variability may be a function of particle selection by suspension feeders (Iken et al., 2001, Bergmann et al., 2009, Jeffreys et al., 2009, Dubois and Colombo, 2014), with smaller particles depleted in heavy isotopes relative to larger particles (Rau et al., 1990; Tyler et al., 1995). However, the spread in the $\delta^{13}C$ values likely represents spatial variability in their food resource (which may be linked to the degree or frequency of resuspension events discussed below), with suspension

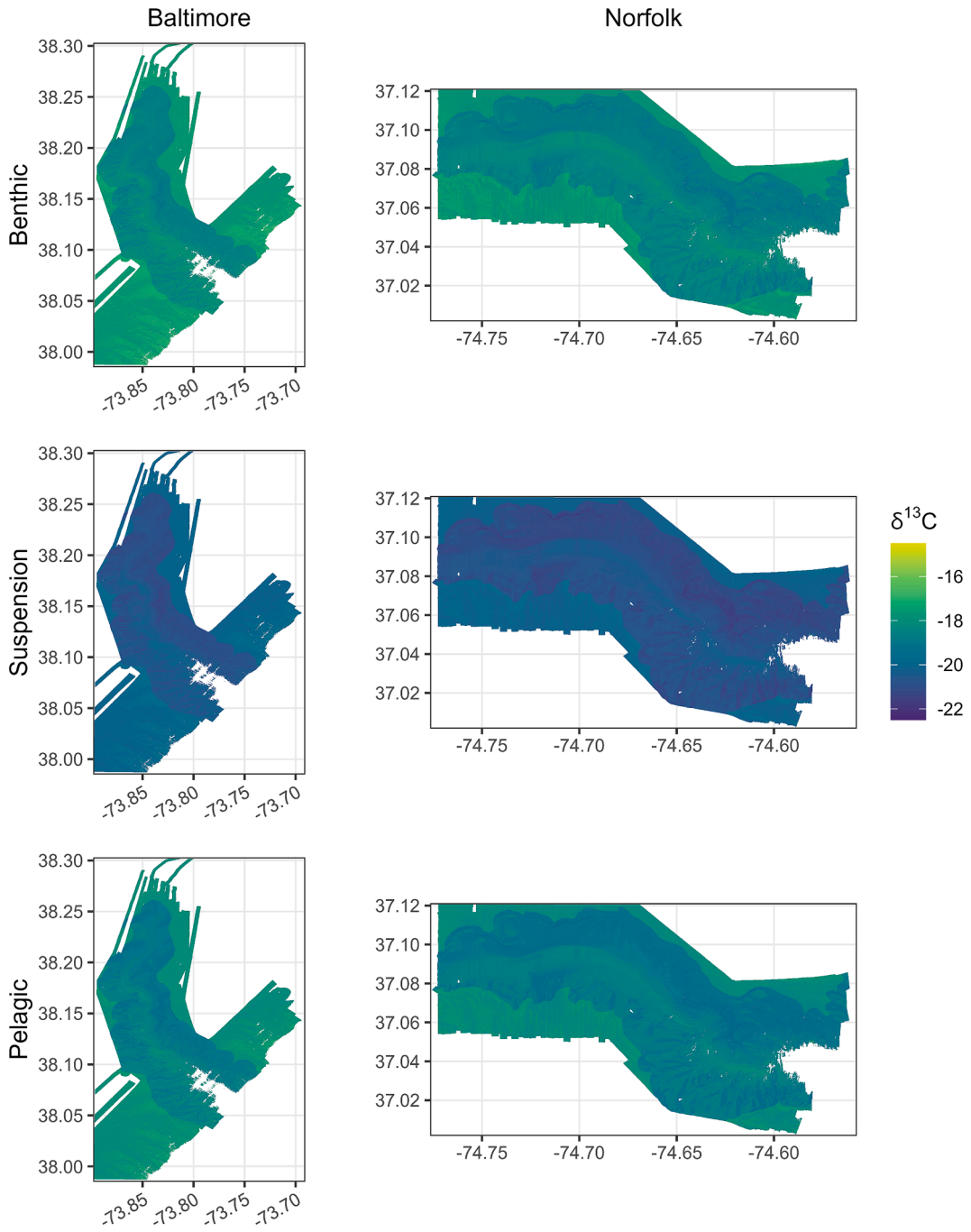

Fig. 6. Isoscapes showing the predicted $\delta^{13}C$ values (‰) from the averaged carbon model for each of the primary feeding groups (Benthic, Pelagic, Suspension) in Baltimore and Norfolk canyons.

feeders residing within the canyon ^{13}C-depleted relative to those found on the slope. While depth has been proposed as more important than location (canyon vs. slope) in driving isotope patterns of consumers (Romero-Romero et al., 2016), conclusions from this previous work were limited by the few data available from non-canyon environments. In contrast, results from our model analysis indicate that both location within the canyon and associated terrain (slope, slope variability, and aspect), as well as depth influence suspension feeder isotopic compositions, and potentially drive niche separation among feeding groups (Figs. 2 and S2, Demopoulos et al., 2017a, b).

The location within the canyon seascape may also influence consumer isotopic composition. For example, after plotting observations of suspension-feeding corals (coral location data previously published in Brooke et al., 2017) within the two canyons (Fig. 8), coral occurrence was tightly associated with the low isotope values predicted by the modeled isoscapes and corresponded to areas of high slope, particularly concentrated along the canyon walls (Fig. 8AB). Suspension feeding corals may be assimilating a mixture of food sources including fresh POM and small zooplankton (Kiriakoulakis et al., 2005; Sherwood et al., 2008; Duineveld et al., 2012; Demopoulos et al., 2017a, b). While some corals had $\delta^{13}C$ values consistent with POM bottom water, they were not ^{15}N-enriched relative to POM (Supplementary Tables 2, 4). Similar species of corals found in Baltimore canyon were also present in Norfolk canyon, including *D. dianthus*, *D. pertusum*, *P. arborea*, and *Anthothela grandiflora*. These animals were isotopically closest to values for surface POM ($\delta^{13}C$: BC: −21.2 ‰ ± 0.5, NC: −21.8 ‰ ± 0.4) and sediment trap

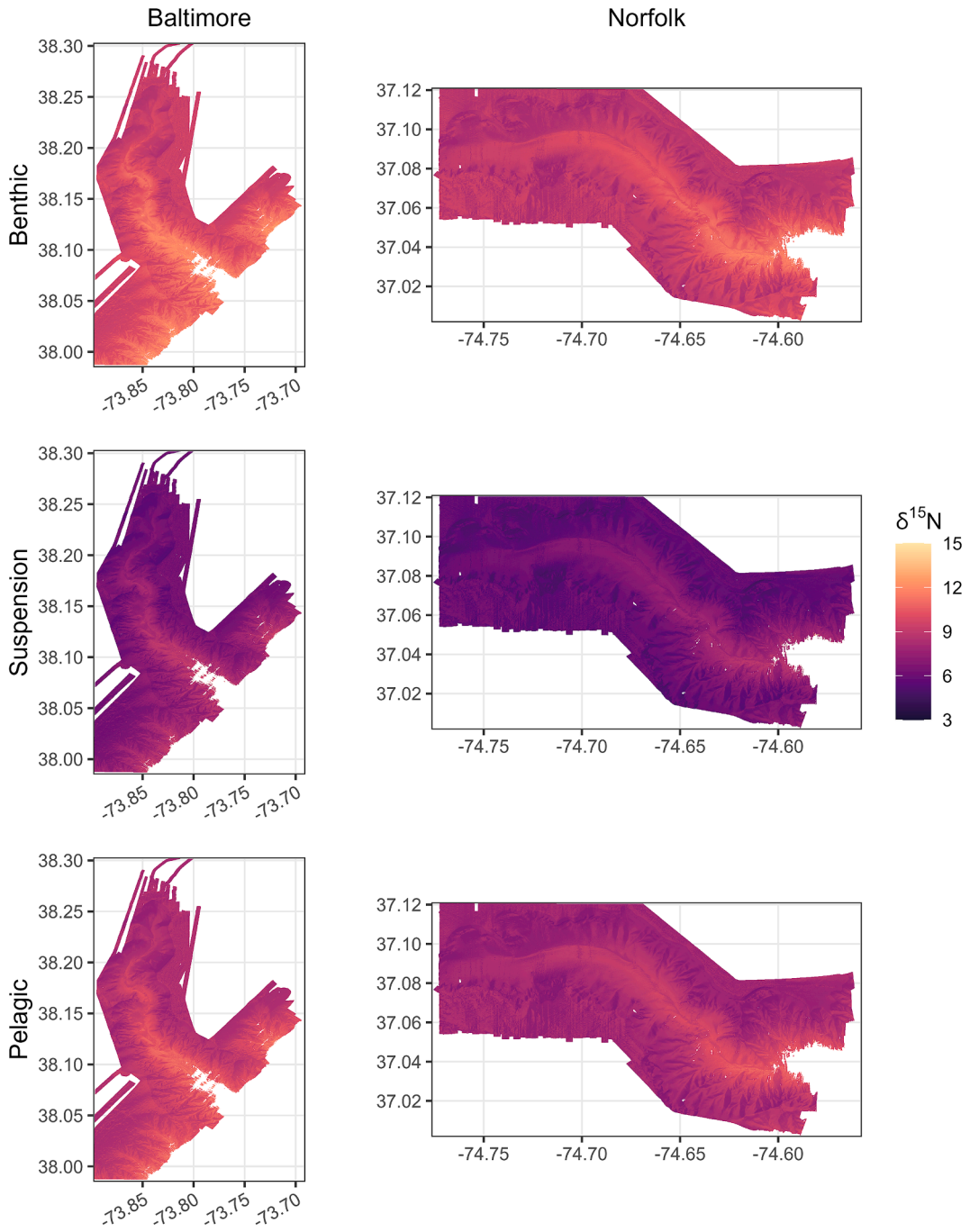

Fig. 7. Isoscapes showing the predicted $\delta^{15}N$ values (‰) from the averaged nitrogen model for each of the primary feeding groups (Benthic, Pelagic, Suspension) in Baltimore and Norfolk canyons.

organic material ($\delta^{13}C$: –22.3 ‰ ± 0.1), indicating that they select fresh material, leading to little isotopic fractionation in the coral tissue relative to surface POM (Sherwood et al., 2008). Cold-water corals have been shown to be associated with areas where topography interacts with hydrography, characterized by internal wave motions and downwelling (De Mol et al., 2011, Howell et al., 2011, Huvenne et al., 2011, Gori et al., 2013, Rengstorf et al., 2013, Robert et al., 2015, Pierdomenico et al., 2016, Fabri et al., 2017, van den Beld et al., 2017, Aslam et al., 2018, Bargain et al., 2018, Pearman et al., 2020), resulting in continuous delivery of this fresh food source (Mohn et al., 2014, Fabri et al., 2017, Lo Iacono et al., 2018). By living on the edge of the canyon walls, these colonies may be bathed in nepheloid layers (Ross et al., 2017) and/or high-quality organic matter transported from the shelf down canyon or deposited from surface production, and less reliant on resuspended, possibly less labile, POM. In contrast, the lower performance of the model within the canyon channel (non-wall) environment may also be a result of the variation in food resources utilized by species in these areas.

The isotopic continuum for coral species present in Norfolk canyon, from low to high $\delta^{13}C$ and $\delta^{15}N$ values, followed the same trend as Baltimore canyon (this study, Demopoulos et al., 2017a, b), with lower values associated with species residing on high-profile hard substrates (e.g., *D. pertusum, P. arborea*) and higher isotope values present in species residing in less dynamic, more quiescent sedimented environments (e.g., *F. alabastrum, Umbellula* sp.) where resuspension events and benthic sources may be more important. High $\delta^{13}C$ values of *F. alabastrum* also may reflect feeding carnivorously on benthic infauna

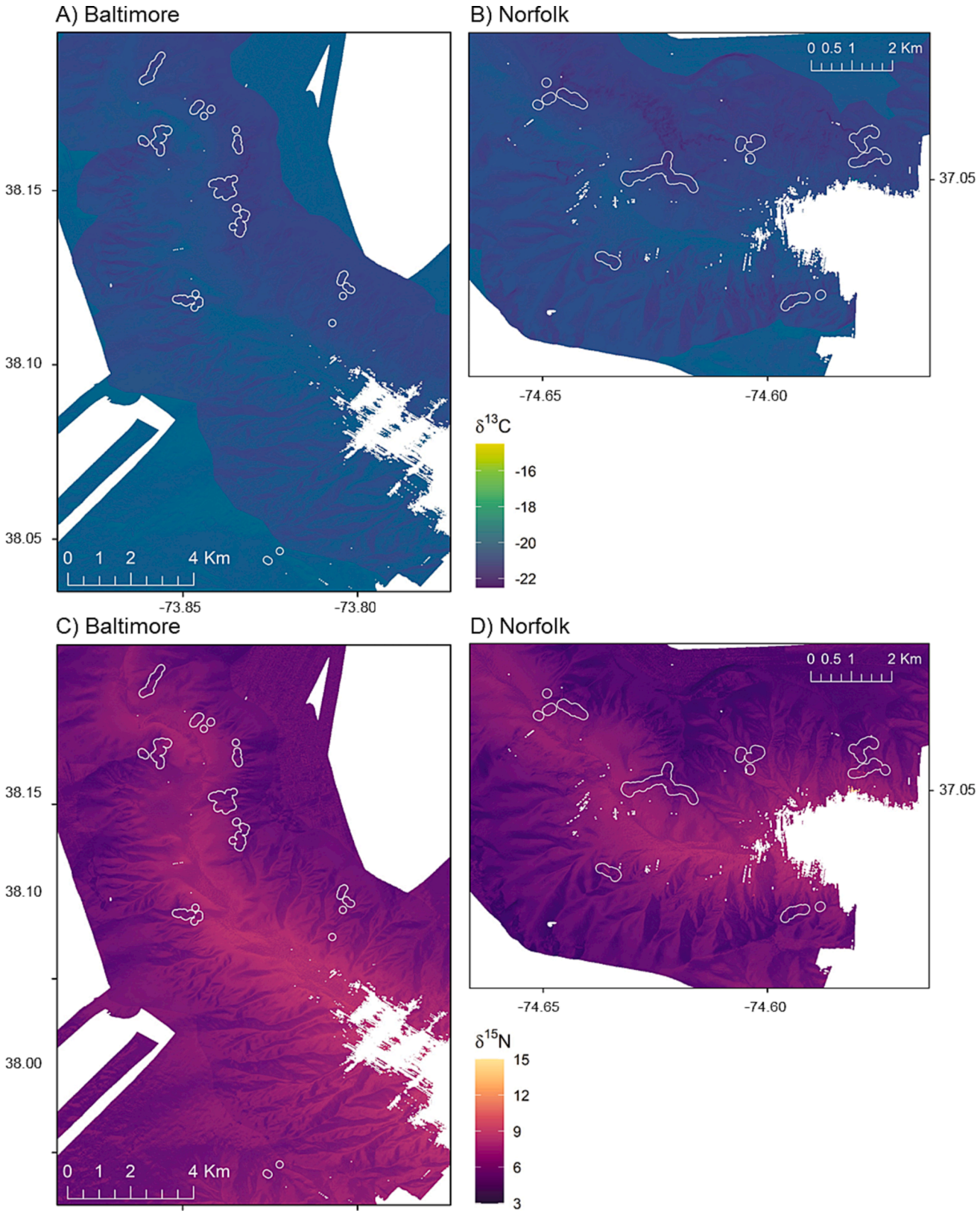

Fig. 8. Suspension-feeder isoscapes of Baltimore (A, C) and Norfolk (B, D) canyons with coral distributions outlined in white. Colors represent the different isotopes with cool colors (blues, greens) for $\delta^{13}C$ data (A, B) and warm colors (pinks, purples) for $\delta^{15}N$ data (C, D), both in ‰.

and demersal zooplankton (Sherwood et al., 2008). The antipatharian *Sibopathes* sp. had the second highest $\delta^{15}N$ (10.4 ‰ ± 0.8) of the suspension feeders, which may represent consumption of degraded organic material and/or higher trophic level organisms, such as zooplankton (Wagner et al., 2012); however, no analyzed zooplankton in the current study had isotope values consistent with $\delta^{13}C$ and $\delta^{15}N$ values of the *Sibopathes*. While it is possible that food resources for this species were not sampled, their higher $\delta^{15}N$ values relative to sympatric corals collected suggest they are potentially feeding at a higher trophic level. *Umbellula* sp. (sea pens) had the highest average $\delta^{13}C$ and $\delta^{15}N$ values of the suspension feeders; all specimens analyzed were collected on the adjacent slope where the consumer isotope values were significantly higher than those within the canyon. Not surprising, *Umbellula* sp. were found on soft substrates at depths (>1,500 m) where POM experiences high isotope fractionation (e.g., Mintenbeck et al., 2007), as a result of microbial induced reworking during settlement and/or isotopic changes during sediment resuspension events.

Benthic feeders occupied the other end of the isotopic spectrum; their higher isotope values were expected because they likely utilize OM that has been reworked and recycled over time (Lopez and Levinton, 1987), leading to enrichment in the heavy isotope. Thus, isotopic differences among benthic feeders may indicate food consumption along a gradient in freshness, from fresh (low $\delta^{13}C/\delta^{15}N$) to degraded (high $\delta^{13}C/\delta^{15}N$, (Jeffreys et al., 2009)); this gradient in freshness may be spatially explicit and influenced by sediment deposition and resuspension areas. Microbial utilization of isotopically light lipids in POM as it descends to the seafloor (or at the seafloor) leads to ^{13}C-enriched OM (Mintenbeck et al., 2007). The subsequent consumption by benthic feeders helps explain the heavy $\delta^{13}C$ values observed in this group in both canyon and slope environments (Demopoulos et al., 2017a). Higher order benthic consumers had stable isotope data that indicate separation among species with similar feeding strategies where the baseline food resource is consistent with carbon derived from photosynthetic material. Additionally, certain taxa exhibit distinct biochemical responses to seasonal changes in quality of phytodetritus, including congeners analyzed in this study (*Amphiura* sp., and *Hyalinoecia* sp. (Jeffreys et al., 2009). This suggests they may modify food selection when resources are limited contributing to variation in isotope values. The higher isotope values of benthic feeders compared to suspension feeders in the canyon environment are consistent with consumption of older, more refractory, isotopically heavy OM. The same pattern was observed in the slope benthic and suspension feeders; however, there was greater isotopic overlap with these two groups suggesting higher similarity in food sources (Fig. 2). Given that the benthic feeding group represents multiple trophic levels, the range in $\delta^{15}N$ could be a function of the different trophic levels represented (from primary consumers to higher-level carnivores), as well as the variability in the source $\delta^{15}N$ from the baseline. It should be noted that feeding group assignments were based on the best available information, which is often limited and not species specific for deep-sea taxa in particular. Feeding modes for certain taxa may change depending on food resource availability, and these changes may influence individual-level isotopic composition. However, by examining isotope patterns and modeled isoscapes by feeding groups that encompass multiple taxa, isotopic separation among feeding groups (benthic, suspension, pelagic) was evident.

Isoscapes developed for pelagic feeders were intermediate between suspension (lower values) and benthic (higher values) feeding groups. Pelagic feeders included several taxa typically found in the mesopelagic zone, including a variety of euphausiid species and decapod shrimp, as well as several species of mesopelagic and bathypelagic fishes. Many of these species are known diel vertical migrators, including *Myctophum affine* and *Diaphus* sp., serving as important transport mechanisms of food from the upper water column to the seafloor and back again (Hidaka et al., 2001, Ashjian et al., 2002). Mesopelagic fishes and invertebrates have been observed in the Mid-Atlantic area to consistently occur near the bottom in areas of topographic highs, including deep-sea corals, canyons, and seamounts (Gartner et al., 2008), as well as in areas of high productivity (e.g., continental slopes, Young and Blaber, 1986, Gartner et al., 2008). Isoscapes of pelagic feeders suggest that they may be feeding on distinct food sources from suspension feeders and benthos, and/or their sources are isotopically variable over the water column. This variability suggests utilization of OM that might include a mixture of fresh OM contributed from surface productivity, as well as isotopically heavy OM (and prey resources) found at depth. Because this group could represent multiple trophic levels (McClain-Counts et al., 2017), spatial variability in the $\delta^{15}N$ isoscape may be a function of multi-trophic level representation.

4.3. Influence of carbon geochemistry on $\delta^{13}C$ spatial variability

Spatial variability in deep-sea fauna $\delta^{13}C$ values can be a function of controls on carbon isotopic composition fixed at the sea surface and as it descends to the seafloor and/or is captured en route. These controls include concentration of specific compounds (CO_3), physiological processes (photosynthesis and respiration), physical characteristics (e.g., sea surface temperatures) and type of phytoplankton (diatoms or dinoflagellates, Ohshimo et al., 2019). Phytoplankton isoscapes from the study region provide a low-resolution perspective of the isotopic composition of the baseline carbon source (Magozzi et al., 2017). In contrast, our isoscapes reveal finer scale carbon isotopic gradients along canyon features, providing higher resolution information on carbon dynamics in these deep-sea environments. The isotopic distinctiveness between canyon and slope environments suggests that the primary food source, surface exported POM, undergoes different degradation pathways in these discrete systems (e.g., Macko et al., 1986), potentially influenced by hydrodynamics, including internal tides, and post depositional processes, including alternating deposition and resuspension events.

Seasonal patterns in the isotopic composition of POM and consumers remains unknown for these canyon environments. Previous work revealed seasonal pulses of OM dominated by vertical and lateral transport within Baltimore canyon (Prouty et al., 2017). For Norfolk canyon, surface POM $\delta^{13}C$ values were higher in May compared to November sampling periods (this study), suggesting possible temporal variability in the baseline carbon isotopic composition, at least in surface waters. However, given the limited available $\delta^{13}C$ from sediment trap data, similar isotopic values from both trap (–22.3 ± 0.1, 4.8 ± 0.1 ‰) and sediment OM (-21.9 ± 0.2 ‰, 5.5 ± 0.4 ‰) (Fig. 2, Table 2) suggest the isotopic composition of deposited POM is similar over time.

4.4. Influence of nitrogen geochemistry on $\delta^{15}N$ spatial variability

Variability of $\delta^{15}N$ values for deep-sea consumers is a function of controls on baseline sources of $\delta^{15}N$, including nitrogen cycling dynamics, as well as trophic level of the consumer. Specific factors that influence baseline $\delta^{15}N$ values include fine-scale controls on hydrography, nutrient chemistry at the surface, and phytoplankton primary production (Graham and Bury, 2019). In the water column, denitrification can lead to increased $\delta^{15}N$ values in the baseline sources, which may then be transferred up the food chain (Vokhshoori and McCarthy, 2014). Within canyon environments, elevated $\delta^{15}N$ values may be tied to higher turbidity associated with presence of nepheloid layers (Puig and Palanques, 1998a, b; Fanelli et al., 2011) via resuspension of the POM. Resuspended material consequently ^{15}N-enriched can then become an important food source. Resuspension processes were evident in the study region, where both canyons exhibited high turbidity and nepheloid layers at certain depths (Robertson et al., 2020), which may have a corresponding impact on the canyon's trophic system.

4.5. Isoscape accuracy and limitations

Isoscapes are static maps of isotopic variability extrapolated over

large areas. They represent a slice of the past, and in this study, illustrate timescales dependent on the tissue turnover of the organisms examined. Isoscapes presented here represent isotopic integration over periods of months, maybe years for some taxa, but not weeks/days (Dattagupta et al., 2004, Hill and McQuaid, 2009); with the primary isotopic data included in the model spatially constrained to areas sampled. However, due to the sample limitations, interannual variability cannot be resolved with the present dataset and would require more frequent sampling throughout the year. However, temporal patterns in the surface and bottom POM samples indicates limited changes over 6 mo – 1 year time frames. By using sentinel consumers, suspension feeders, to build our isoscapes, we used the animals to integrate the isotopic variability over time, including short-term or seasonal variability.

Submarine canyons can be challenging environments to map from surface vessels at the resolutions required for meaningful statistical analysis of derivative datasets due to the steep and narrow terrain and variable water column structure that impacts sound velocity. Acquisition artifacts, under sampling of the seafloor due to complex terrain, and smoothing of resultant interpolated bathymetric surfaces can all significantly impact the quality of the extracted terrain variables. Some of these issues were overcome via identification and correlation of significant outliers in the extracted variables with known artifacts and the use of multiple data resolutions (10 and 25 m) for the analysis.

Currently, isoscape models have employed a variety of statistical approaches, including simple interpolation (e.g., kriging), linear regression, general additive models, frequentist mixed modeling, and Bayesian hierarchical spatial modeling (e.g., INLA, St John Glew et al., 2019) of sample data. Many of these are complex models that require long computational times to fit. Our linear models rely on covariates - including a suite of environmental variables (i.e., terrain factors), feeding groups, and zones – to capture the spatial pattern in the data. The resulting models yielded robust results, with negligible residual spatial autocorrelation (Fig. S3) and precise estimates for the modeled isoscapes (Fig. S4 and S5), and good performance under validation (Fig. S6) – without a large computational burden. Compared to purely phenomenological approaches, e.g., ordinary kriging, our regression models also allow inference on the mechanisms driving the observed spatial pattern. However, the ability to extrapolate the model predictions to other areas will require additional data from the region of interest to validate the model. Some of these relationships may exhibit mechanistic context dependence (Catford et al., 2022), and future work in new areas will provide information required to quantify these patterns, enabling generalizations about how deep-sea physical structure influences flux of nutrients and assimilation pathways.

5. Conclusions

In conclusion, to our knowledge, this study represents the first empirical isoscapes of deep-sea environments that predict $\delta^{13}C$ and $\delta^{15}N$ values for different functional groups and identified some underlying mechanistic controls on these patterns in submarine canyons and adjacent slopes. Analysis of the stable isotope variability coupled with measures of seafloor environmental parameters as proxies for habitat heterogeneity and complexity provide insights into mechanistic factors that help influence the trophic diversity and food webs in the mid-Atlantic canyon region. By using the animals to sample the environment, they assimilate a time-integrated isotopic signal, which allows the creation of unique isoscapes based on feeding groups. The models identify several possible environmental controls on ecosystem processes (e.g., food quality, transfer of energy) and associated isotopic baselines. By using low-trophic level consumers (suspension feeders) the isoscapes can be used to evaluate locations for migratory species. There is a suite of migratory marine mammals, as well as commercially important fishes and invertebrates that utilized the Atlantic canyons seasonally, as well as throughout their life histories. The deep-sea isoscapes presented here could be used to test resource use and locality for these species.

This study represents an initial step in characterizing the geospatial isodynamics for feeding groups, with concomitant mechanistic controls (slope, etc.) within deep-sea environments. Given the significance of slope, slope variability, and aspect, as well as depth, it appears that canyon morphology, habitat heterogeneity, and depositional dynamics may play a role in diversifying associated food webs and niche specialization identified for consumers. Our deep-sea isoscapes from two canyon systems provide a starting point from which to test whether observed patterns are broadly generalizable to multiple canyon environments or if they are more site specific and a function of canyon morphology. In addition, they provide a baseline for monitoring variability in the quality and quantity of surface primary production associated with climate change and the consequential impact to benthic communities, which play critical roles in carbon cycling in our world's oceans.

CRediT authorship contribution statement

Amanda W.J. Demopoulos: Conceptualization, Formal analysis, Investigation, Methodology, Validation, Visualization, Writing – original draft, Funding acquisition, Project administration, Writing – review & editing. **Brian J. Smith:** Conceptualization, Formal analysis, Methodology, Validation, Visualization, Writing – original draft, Writing – review & editing. **Jill R. Bourque:** Conceptualization, Investigation, Methodology, Visualization, Writing – original draft, Writing – review & editing. **Jason D. Chaytor:** Conceptualization, Formal analysis, Investigation, Validation, Visualization, Writing – original draft, Writing – review & editing. **Jennifer McClain-Counts:** Data curation, Formal analysis, Investigation, Methodology, Visualization, Writing – original draft, Writing – review & editing. **Nancy Prouty:** Investigation, Methodology, Writing – original draft, Writing – review & editing. **Steve W. Ross:** Funding acquisition, Investigation, Project administration, Writing – review & editing. **Sandra Brooke:** Funding acquisition, Investigation, Validation, Writing – review & editing. **Gerard Duineveld:** Conceptualization, Investigation, Methodology, Writing – review & editing. **Furu Mienis:** Conceptualization, Investigation, Methodology, Validation, Writing – review & editing.

Declaration of competing interest

The authors declare that they have no known competing financial interests or personal relationships that could have appeared to influence the work reported in this paper.

Data availability

All raw data and metadata can be found on Sciencebase: https://doi.org/10.5066/F71N7Z9R; https://doi.org/10.5066/F7RJ4HD2; and https://doi.org/10.5066/P955FYVL.

Acknowledgments

This project resulted from a joint partnership with USGS, NOAA Office of Ocean Exploration and Research (OER), and BOEM within the National Oceanographic Partnership Program (NOPP), joined by academic and private partners. A.W.J.D. was funded by the USGS Environments Program, currently known as the Land Management Research Program (Project #BA09FFV). S.B. and S.W.R. were funded by the Bureau of Ocean Energy Management (BOEM) through a contract from CSA Ocean Sciences, Inc. (contract M10PC00100). We thank G. Brewer, C. Charles, M. Khalil, L. Ball (USGS), G. Boland (BOEM), S. Viada (CSA), and K. Cantwell (NOAA-OER) for support throughout this project. Thanks to M. Lavaleye and M. Rhode for their assistance at sea, and to R. Lee, WSU, for isotope analysis. Funding for NOAA ships, ROVs, and data management were provided by the NOAA OER. We thank the ship and shore-based personnel and all the science and outreach personnel for

their hard work during the cruises. We are particularly grateful to C. Mah, C. Robertson, and the many other taxonomic experts that assisted with this complex study. We are also grateful to B. Fry for fruitful discussions throughout the development of our deep-sea isoscapes, A. Davies for thoughtful comments on an earlier version of this manuscript, as well as the anonymous reviewers for providing input that ultimately improved the final version. Any use of trade, firm, or product names is for descriptive purposes only and does not imply endorsement by the U. S. Government.

Appendix A. Supplementary data

Supplementary data to this article can be found online at https://doi.org/10.1016/j.pocean.2024.103231.

References

Andrews, B.D., Chaytor, J.D., ten Brink, U.S., Brothers, D.S., Gardner, J.V., Lobecker, E. A., Calder, B.R., 2016. Bathymetric terrain model of the Atlantic margin for marine geological investigations (ver. 2.0, May 2016), U.S. Geological Survey Open-File Report 2012–1266, 12 p., 1 pl., https://doi.org/10.3133/ofr20121266.

Arnoldi, N.S., Litvin, S.Y., Madigan, D.J., Micheli, F., Carlisle, A., 2023. Multi-taxa marine isoscapes provide insight into large-scale trophic dynamics in the North Pacific. Prog. Oceanogr. 213.

Ashjian, C.J., Smith, S.L., Flagg, C.N., Idrisi, N., 2002. Distribution, annual cycle, and vertical migration of acoustically derived biomass in the Arabian Sea during 1994–1995. Deep-Sea Research Part II-Topical Studies in Oceanography 49, 2377–2402.

Aslam, T., Hall, R.A., Dye, S.R., 2018. Internal tides in a dendritic submarine canyon. Prog. Oceanogr. 169, 20–32.

Baker, K.D., Wareham, V.E., Snelgrove, P.V.R., Haedrich, R.L., Fifield, D.A., Edinger, E. N., Gilkinson, K.D., 2012. Distributional patterns of deep-sea coral assemblages in three submarine canyons off Newfoundland, Canada. Mar. Ecol. Prog. Ser. 445, 235–249.

Bargain, A., Foglini, F., Pairaud, I., Bonaldo, D., Carniel, S., Angeletti, L., Taviani, M., Rochette, S., Fabri, M.C., 2018. Predictive habitat modeling in two Mediterranean canyons including hydrodynamic variables. Prog. Oceanogr. 169, 151–168.

Barton, K. 2018. MuMIn: Multi-Model Inference. R package version 1.40.4. https://CRAN.R-project.org/package=MuMIn.

Bergmann, M., Dannheim, J., Bauerfeind, E., Klages, M., 2009. Trophic relationships along a bathymetric gradient at the deep-sea observatory HAUSGARTEN. Deep-Sea Research Part I-Oceanographic Research Papers 56, 408–424.

Bianchelli, S., Gambi, C., Pusceddu, A., Danovaro, R., 2008. Trophic conditions and meiofaunal assemblages in the Bari canyon and the adjacent open slope (Adriatic Sea). Chem. Ecol. 24, 101–109.

Bjørnstad, O. N. 2019. ncf: Spatial Nonparametric Covariance Functions, R package version 1.2-8.

Bosman, S.H., Schwing, P.T., Larson, R.A., Wildermann, N.E., Brooks, G.R., Romero, I.C., Sanchez-Cabeza, J.A., Ruiz-Fernandez, A.C., Machain-Castillo, M.L., Gracia, A., Escobar-Briones, E., Murawski, S.A., Hollander, D.J., 2020. The southern Gulf of Mexico: A baseline radiocarbon isoscape of surface sediments and isotopic excursions at depth. PloS One (15).

Bowen, G.J., 2010. Isoscapes: spatial pattern in isotopic biogeochemistry. Annu. Rev. Earth Planet. Sci. 38 (38), 161–187.

Bowen, G.J., Hoogewerff, J., 2009. Isoscapes: Isotope mapping and its applications. J. Geochem. Explor. 102, 5–7. https://doi.org/10.1016/j.gexplo.2009.05.001.

Brault, E.K., Koch, P.L., McMahon, K.W., Broach, K.H., Rosenfield, A.P., Sauthoff, W., Loeb, V.J., Arrigo, K.R., Smith, W.O., 2018. Carbon and nitrogen zooplankton isoscapes in West Antarctica reflect oceanographic transitions. Mar. Ecol. Prog. Ser. 593, 29–45.

Brooke, S.D., Watts, M.W., Heil, A.D., Rhode, M., Mienis, F., Duineveld, G.C.A., Davies, A.J., Ross, S.W., 2017. Distributions and habitat associations of deep-water corals in Norfolk and Baltimore canyons, mid-Atlantic bight, USA. Deep Sea Res. Part II 137, 131–147.

Carpenter-Kling, T., Pistorius, P., Reisinger, R., Cherel, Y., Connan, M., 2020. A critical assessment of marine predator isoscapes within the southern Indian Ocean. movement. Ecology 8.

Cartes, J.E., Sorbe, J.C., 1999. Estimating secondary production in bathyal suprabenthic peracarid crustaceans from the Catalan Sea slope (western Mediterranean; 391–1255 m). J. Exp. Mar. Biol. Ecol. 239, 195–210.

Cartes, J.E., Fanelli, E., Papiol, V., Maynou, F., 2010. Trophic relationships at intrannual spatial and temporal scales of macro and megafauna around a submarine canyon off the catalonian coast (western Mediterranean). J. Sea Res. 63, 180–190.

Cartes, J.E., Fanelli, E., Kapiris, K., Bayhan, Y.K., Ligas, A., Lopez-Perez, C., Murenu, M., Papiol, V., Rumolo, P., Scarcella, G., 2014. Spatial variability in the trophic ecology and biology of the deep-sea shrimp *Aristaeomorpha foliacea* in the Mediterranean Sea. Deep-Sea Research Part I-Oceanographic Research Papers 87, 1–13.

Cartes, J.E., Sorbe, J.C., 1998. Aspects of population structure and feeding ecology of the deep-water mysid *Boreomysis arctica*, a dominant species in western Mediterranean slope assemblages. J. Plankton Res. 20, 2273–2290.

Catford, J.A., Wilson, J.R.U., Pysek, P., Hulme, P.E., Duncan, R.P., 2022. Addressing context dependence in ecology. Trends Ecol. Evol. 37, 158–170.

Chauvet, P., Metaxas, A., Hay, A.E., Matabos, M., 2018. Annual and seasonal dynamics of deep-sea megafaunal epibenthic communities in Barkley canyon (British Columbia, Canada): a response to climatology, surface productivity and benthic boundary layer variation. Prog. Oceanogr. 169, 89–105.

Cheesman, A.W., Cernusak, L.A., 2016. Isoscapes: a new dimension in community ecology. Tree Physiol. 36, 1456–1459.

Cunha, M.R., Paterson, G.L.J., Amaro, T., Blackbird, S., de Stigter, H.C., Ferreira, C., Glover, A., Hilario, A., Kiriakoulakis, K., Neal, L., Ravara, A., Rodrigues, C.F., Tiago, A., Billett, D.S.M., 2011. Biodiversity of macrofaunal assemblages from three portuguese submarine canyons (NE Atlantic). Deep-Sea Research Part II-Topical Studies in Oceanography 58, 2433–2447.

Dattagupta, S., Bergquist, D.C., Szalai, E.B., Macko, S.A., Fisher, C.R., 2004. Tissue carbon, nitrogen, and sulfur stable isotope turnover in transplanted bathymodiolus childressi mussels: relation to growth and physiological condition. Limnol. Oceanogr. 49, 1144–1151.

De Leo, Smith, C.R., Rowden, A.A., Bowden, D.A., 2010. Submarine canyons: hotspots of benthic biomass and productivity in the deep sea. Proceedings of the Royal Society B-Biological Sciences 277, 2783–2792. https://doi.org/10.1098/rspb.2010.0462.

De Mol, L., Van Rooij, D., Pirlet, H., Greinert, J., Frank, N., Quemmerais, F., Henriet, J.P., 2011. Cold-water coral habitats in the penmarc'h and guilvinec canyons (Bay of Biscay): deep-water versus shallow-water settings. Mar. Geol. 282, 40–52.

deBruyn, A., Meeuwigg, J., 2001. Detecting lunar cycles in marine ecology: periodic regression versus categorical ANOVA. Mar. Ecol. Prog. Ser. 214, 307–310.

Dell'Anno, A., Pusceddu, A., Corinaldesi, C., Canals, M., Heussner, S., Thomsen, L., Danovaro, R., 2013. Trophic state of benthic deep-sea ecosystems from two different continental margins off Iberia. Biogeosciences 10, 2945–2957.

Demopoulos, A.W.J., Cormier, N., Ewel, K., Fry, B., 2008. Use of multiple chemical tracers to define habitat use of Indo-Pacific mangrove crab, *Scylla serrata* (Decapoda: Portunidae). Estuar. Coasts 31, 371–381.

Demopoulos, A.W.J., McClain-Counts, J., Ross, S.W., Brooke, S., Mienis, F., 2017a. Food-web dynamics and isotopic niches in deep-sea communities residing in a submarine canyon and on the adjacent open slopes. Mar. Ecol. Prog. Ser. 578, 19–33.

Demopoulos, A.W.J., McClain Counts, J.P., Ross, S., Brooke, S., and Rhode, M., 2017b, Chapter 16: Food-web structure in canyon and slope-associated fauna revealed by stable isotopes, In CSA Ocean Sciences Inc., eds., Exploration and Research of Mid-Atlantic Deepwater Hard Bottom Habitats and Shipwrecks with Emphasis on Canyons and Coral Communities: Atlantic Deepwater Canyons Study. Sterling (VA): U.S. Department of the Interior, Bureau of Ocean Energy Management, Atlantic OCS Region. OCS Study BOEM 2017-060. 1000 p. +apps.

Demopoulos, A.W.J., McClain-Counts, J.P., Ross, S.W., Brooke, S., Mienis, F., 2017c. Food-web dynamics and isotopic niches in deep-sea communities residing in a submarine canyon and on the adjacent open slopes. US Geological Survey Data Release. https://doi.org/10.5066/F71N7Z9R.

Demopoulos, A.W.J., McClain-Counts, J.P., Bourque, J.R., Chaytor, J., Smith, B.J., Prouty, N.P., Ross, S.W., Brooke, S., Duineveld, G., Mienis, F., 2024. Stable isotope data and terrain variables for isoscape modeling around two submarine canyons in the western Atlantic sampled in 2012–2013. U.S. Geological Survey Data Release. https://doi.org/10.5066/P955FYVL.

Dubois, S.F., Colombo, F., 2014. How picky can you be? temporal variations in trophic niches of co-occurring suspension-feeding species. Food Webs 1, 1–9.

Duineveld, G.C.A., Jeffreys, R.M., Lavaleye, M.S.S., Davies, A.J., Bergman, M.J.N., Watmough, T., Witbaard, R., 2012. Spatial and tidal variation in food supply to shallow cold-water coral reefs of the mingulay reef complex (outer Hebrides, Scotland). Mar. Ecol. Prog. Ser. 444, 97–115.

Duineveld, G., Lavaleye, M., Berghuis, E., de Wilde, P., 2001. Activity and composition of the benthic fauna in the Whittard canyon and the adjacent continental slope (NE Atlantic). Oceanol. Acta 24, 69–83.

Durante, L.M., Smith, R.O., Kolodzey, S., McMullin, R.M., Salmond, N.H., Schlieman, C. D., O'Connell-Milne, S.A., Frew, R.D., Van Hale, R., Wing, S.R., 2021. Oceanographic transport along frontal zones forms carbon, nitrogen, and oxygen isoscapes on the east coast of New Zealand: implications for ecological studies. Cont. Shelf Res. 216.

Fabri, M.C., Bargain, A., Pairaud, I., Pedel, L., Taupier-Letage, I., 2017. Cold-water coral ecosystems in Cassidaigne Canyon: an assessment of their environmental living conditions. Deep-Sea Research Part II-Topical Studies in Oceanography 137, 436–453.

Fanelli, E., Papiol, V., Cartes, J.E., Rumolo, P., Brunet, C., Sprovieri, M., 2011. Food web structure of the epibenthic and infaunal invertebrates on the Catalan Slope (NW Mediterranean). Evidence from δ13C and δ15N Analysis, Deep-Sea Research I 58, 98–109.

Fanelli, E., Papiol, V., Cartes, J.E., Rumolo, P., Lopez-Perez, C., 2013. Trophic webs of deep-sea megafauna on mainland and insular slopes of the NW Mediterranean: a comparison by stable isotope analysis. Mar. Ecol. Prog. Ser. 490, 199–221.

Farre, J.A., McGregor, B.A., Ryan, W.B., Robb, J.M., 1983. Breaching the shelfbreak: passage from youthful to mature phase in submarine canyon evolution.*in* D. In: Stanley, J., Moore, G.T. (Eds.), The Shelfbreak: Critical Interface on Continental Margins. SEPM Society for Sedimentary Geology.

Gage, J.D., Tyler, P.A., 1991. Deep-Sea biology: a natural history of organisms at the Deep-Sea floor. Cambridge University Press.

Gardner, W.D., 1989a. Baltimore canyon as a modern conduit of sediment to the Deep Sea. Deep sea research part a. Oceanographic Research Papers 36, 323–358.

Gardner, W.D., 1989b. Periodic resuspension in Baltimore canyon by focusing of intemal waves. J. Geophys. Res. 94, 18185–18194.

Gartner, J.V., Sulak, K.J., Ross, S.W., Necaise, A.M., 2008. Persistent near-bottom aggregations of mesopelagic animals along the North Carolina and Virginia continental slopes. Mar. Biol. 153, 825–841.
Gibbs, M., Leduc, D., Nodder, S.D., Kingston, A., Swales, A., Rowden, A.A., Mountjoy, J., Olsen, G., Ovenden, R., Brown, J., Bury, S., Graham, B., 2020. Novel application of a compound-specific stable isotope (CSSI). Tracking Technique Demonstrates Connectivity between Terrestrial and Deep-Sea Ecosystems via Submarine Canyons. Frontiers in Marine Science 7.
Gori, A., Orejas, C., Madurell, T., Bramanti, L., Martins, M., Quintanilla, E., Marti-Puig, P., Lo Iacono, C., Puig, P., Requena, S., Greenacre, M., Gili, J.M., 2013. Bathymetrical distribution and size structure of cold-water coral populations in the cap de creus and lacaze-duthiers canyons (northwestern Mediterranean). Biogeosciences 10, 2049–2060.
Graham, B., Bury, S., 2019. Marine Isoscapes for trophic and animal movement studies in the southwest Pacific Ocean. New Zealand Aquatic Environment and Biodiversity Report No. 218, ISSN 1179-6480 (online), ISBN 978-0-9951269-2-3 (online).
Haalboom, S., de Stigter, H., Duineveld, G., van Haren, H., Reichart, G.J., Mienis, F., 2021. Suspended particulate matter in a submarine canyon (Whittard Canyon, Bay of Biscay, NE Atlantic Ocean): assessment of commonly used instruments to record turbidity. Mar. Geol. 434.
Harris, P.T., Whiteway, T., 2011. Global distribution of large submarine canyons: geomorphic differences between active and passive continental margins. Mar. Geol. 285, 69–86.
Hellmann, C., Werner, C., 2016. A Spatially Explicit Dual-Isotope Approach to Map Regions of Plant-Plant Interaction after Exotic Plant Invasion. PloS One 11. https://doi.org/10.1371/journal.pone.0159403.
Hidaka, K., Kawaguchi, K., Murakami, M., Takahashi, M., 2001. Downward transport of organic carbon by diel migratory micronekton in the western equatorial Pacific: its quantitative and qualitative importance. Deep-Sea Research Part I-Oceanographic Research Papers 48, 1923–1939.
Hill, J.M., McQuaid, C.D., 2009. Effects of food quality on tissue-specific isotope ratios in the mussel Perna perna. Hydrobiologia 635, 81–94.
Ho, P.C., Okuda, N., Yeh, C.F., Wang, P.L., Gong, G.C., Hsieh, C.H., 2021. Carbon and nitrogen isoscape of particulate organic matter in the East China Sea. Prog. Oceanogr. 197. https://doi.org/10.1016/j.pocean.2021.102667.
Hoffman, J.C., Sutton, T.T., 2010. Lipid correction for carbon stable isotope analysis of deep-sea fishes. Deep-Sea Research. Part I, Oceanographic Research Papers 57, 956–964.
Howell, K.L., Holt, R., Endrino, I.P., Stewart, H., 2011. When the species is also a habitat: comparing the predictively modelled distributions of *Lophelia pertusa* and the reef habitat it forms. Biol. Conserv. 144, 2656–2665.
Hutchinson, G.E., 1957. Concluding remarks. Cold Spring Harb. Symp. Quant. Biol. 22, 415–427.
Hutchinson, G.E., 1978. An introduction to population ecology. Yale University Press, New Haven.
Huvenne, V.A.I., Tyler, P.A., Masson, D.G., Fisher, E.H., Hauton, C., Hühnerbach, V., Le Bas, T.P., Wolff, G.A., 2011. A picture on the wall: innovative mapping reveals cold-water coral refuge in submarine canyon. PLoS One 6, e28755.
Iken, K., Brey, T., Wand, U., Voigt, J., Junghans, P., 2001. Food web structure of the benthic community at the porcupine abyssal plain (NE Atlantic): a stable isotope analysis. Prog. Oceanogr. 50, 383–405.
Inthorn, M., Wagner, T., Scheeder, G., Zabel, M., 2006. Lateral transport controls distribution, quality, and burial of organic matter along continental slopes in high-productivity areas. Geology 34, 205–208.
Jeffreys, R.M., Wolff, G.A., Murty, S.J., 2009. The trophic ecology of key megafaunal species at the Pakistan margin: evidence from stable isotopes and lipid biomarkers. Deep-Sea Research Part I-Oceanographic Research Papers 56, 1816–1833.
Jenness, J. DEM Surface Tools for ArcGIS (surface_area.exe). Jenness Enterprises. http://www.jennessent.com/arcgis/surface_area.htm.
Jennings, S., Warr, K.J., 2003. Environmental correlates of large-scale spatial variation in the $\delta^{15}N$ of marine animals. Mar. Biol. 142, 1131–1140.
Jones, D.O.B., Yool, A., Wei, C.L., Henson, S.A., Ruhl, H.A., Watson, R.A., Gehlen, M., 2014. Global reductions in seafloor biomass in response to climate change. Glob. Chang. Biol. 20, 1861–1872.
Kiriakoulakis, K., Fisher, E., Wolff, G.A., Freiwald, A., Grehan, A., Roberts, J.M., 2005. Lipids and nitrogen isotopes of two deep-water corals from the north-East Atlantic: initial results and implications for their nutrition. In: Freiwald, A., Roberts, J.M. (Eds.), Cold-Water Corals and Ecosytems. Springer-Verlag, Berlin Heidelberg, pp. 715–729.
Kiriakoulakis, K., Blackbird, S., Ingels, J., Vanreusel, A., Wolff, G.A., 2011. Organic geochemistry of submarine canyons: the portuguese margin. Deep-Sea Research Part II-Topical Studies in Oceanography 58, 2477–2488.
Klages, M., Boetius, A., Christensen, J.P., Deubel, H., Piepenburg, D., Schewe, I., Soltwedel, T., 2003. The benthos of Arctic seas and its role for the carbon cycle at the seafloor. In: Stein, R., Macdonald, R.W. (Eds.), The Organic Carbon Cycle in the Arctic Ocean. Springer, Heidelberg, pp. 139–167.
Lo Iacono, C., Robert, K., Gonzalez-Villanueva, R., Gori, A., Gili, J.M., Orejas, C., 2018. Predicting cold-water coral distribution in the cap de creus canyon (NW Mediterranean): implications for marine conservation planning. Prog. Oceanogr. 169, 169–180.
Lopez, G.R., Levinton, J.S., 1987. Ecology of deposit-feeding animals in marine sediments. Q. Rev. Biol. 62, 235–260.
Lorrain, A., Graham, B.S., Popp, B.N., Allain, V., Olson, R.J., Hunt, B.P.V., Potier, M., Fry, B., Galvan-Magana, F., Menkes, C.E.R., Kaehler, S., Menard, F., 2015. Nitrogen isotopic baselines and implications for estimating foraging habitat and trophic position of yellowfin tuna in the indian and pacific oceans. Deep-Sea Research Part II-Topical Studies in Oceanography 113, 188–198.
Macko, S.A., Estep, M.L.F., Engel, M.H., Hare, P.E., 1986. Kinetic fractionation of stable nitrogen isotopes during amino-acid transamination. Geochim. Cosmochim. Acta 50, 2143–2146.
Magozzi, S., Yool, A., Zanden, H.B.V., Wunder, M.B., Trueman, C.N., 2017. Using ocean models to predict spatial and temporal variation in marine carbon isotopes. Ecosphere 8.
Mamouridis, V., Cartes, J.E., Parra, S., Fanelli, E., Salinas, J.I.S., 2011. A temporal analysis on the dynamics of deep-sea macrofauna: influence of environmental variability off Catalonia coasts (western Mediterranean). Deep-Sea Research Part I-Oceanographic Research Papers 58, 323–337.
McClain, C.R., Barry, J.P., 2010. Habitat heterogeneity, disturbance, and productivity work in concert to regulate biodiversity in deep submarine canyons. Ecology 91, 964–976.
McClain-Counts, J.P., Demopoulos, A.W.J., Ross, S.W., 2017. Trophic structure of mesopelagic fishes in the Gulf of Mexico revealed by gut content and stable isotope analyses. Mar. Ecol. 38.
McClain-Counts, J. P., A. W. Demopoulos, S. W. Ross, S. Brooke, and M. Rhode. 2018. Food-web structure of canyon and slope associated fauna revealed by stable isotopes. U.S. Geological Survey Data Release, https://doi.org/10.5066/F7RJ4HD2.
McMahon, K.W., Hamady, L.L., Thorrold, S.R., 2013. A review of ecogeochemistry approaches to estimating movements of marine animals. Limnol. Oceanogr. 58, 697–714.
Mienis, F., Duineveld, G.C.A., Roark, B., Demopoulos, A.W.J., Prouty, N., Campbell-Swarzenski, P., Rhode, M., Brooke, S., Ross, S.W., 2017. Chapter 6: Geological Studies. In CSA Ocean Sciences Inc., eds., Exploration and Research of Mid-Atlantic Deepwater Hard Bottom Habitats and Shipwrecks with Emphasis on Canyons and Coral Communities: Atlantic Deepwater Canyons Study. Sterling (VA): U.S. Department of the Interior, Bureau of Ocean Energy Management, Atlantic OCS Region. OCS Study BOEM 2017-060. 1000 p. +apps.
Mintenbeck, K., Jacob, U., Knust, R., Arntz, W.E., Brey, T., 2007. Depth-dependence in stable isotope ratio $d^{15}N$ of benthic POM consumers: the role of particle dynamics and organism trophic guild. Deep-Sea Research Part I-Oceanographic Research Papers 54, 1015–1023.
Mohn, C., Rengstorf, A., White, M., Duineveld, G., Mienis, F., Soetaert, K., Grehan, A., 2014. Linking benthic hydrodynamics and cold-water coral occurrences: a high-resolution model study at three cold-water coral provinces in the NE Atlantic. Prog. Oceanogr. 122, 92–104.
Navarro, J., Coll, M., Somes, C.J., Olson, R.J., 2013. Trophic niche of squids: insights from isotopic data in marine systems worldwide. Deep-Sea Research Part II-Topical Studies in Oceanography 95, 93–102.
Obelcz, J., Brothers, D., Chaytor, J., Brink, U.t., Ross, S.W., Brooke, S., 2014. Geomorphic characterization of four shelf-sourced submarine canyons along the U.S. mid-Atlantic continental margin. Deep Sea Res. Part II 104, 106–119.
Ohshimo, S., Madigan, D.J., Kodama, T., Tanaka, H., Komoto, K., Suyama, S., Ono, T., Yamakawa, T., 2019. Isoscapes reveal patterns of $\delta^{13}C$ and $\delta^{15}N$ of pelagic forage fish and squid in the Northwest Pacific Ocean. Prog. Oceanogr. 175, 124–138.
Papiol, V., Cartes, J.E., Fanelli, E., Rumolo, P., 2013. Food web structure and seasonality of slope megafauna in the NW Mediterranean elucidated by stable isotopes: relationship with available food sources. J. Sea Res. 77, 53–69.
Pearman, T.R.R., Robert, K., Callaway, A., Hall, R., Lo Iacono, C., 2020. Improving the predictive capability of benthic species distribution models by incorporating oceanographic data - Towards holistic ecological modelling of a submarine canyon. Prog. Oceanogr. 184. https://doi.org/10.1016/j.pocean.2020.102338.
Pierdomenico, M., Martorelli, E., Dominguez-Carrio, C., Gili, J.M., Chiocci, F.L., 2016. Seafloor characterization and benthic megafaunal distribution of an active submarine canyon and surrounding sectors: the case of gioia canyon (southern Tyrrhenian Sea). J. Mar. Syst. 157, 101–117.
Pinnegar, J.K., Polunin, N.V.C., 1999. Differential fractionation of $\delta^{13}C$ and $\delta^{15}N$ among fish tissues: implications for the study of trophic interactions. Funct. Ecol. 13, 225–231.
Post, D.M., Layman, C.A., Arrington, D.A., Takimoto, G., Quattrochi, J., Montana, C.G., 2007. Getting to the fat of the matter: models, methods and assumptions for dealing with lipids in stable isotope analyses. Oecologia 152, 179–189.
Prouty, N.G., Mienis, F., Campbell-Swarzenski, P., Roark, E.B., Davies, A.J., Robertson, C. M., Duineveld, G., Ross, S.W., Rhode, M., Demopoulos, A.W.J., 2017. Seasonal variability in the source and composition of particulate matter in the depositional zone of Baltimore canyon, U.S. mid-Atlantic bight. Deep Sea Res. Part I 127, 77–89.
Puig, P., Palanques, A., 1998a. Nepheloid structure and hydrographic control on the Barcelona continental margin, northwestern Mediterranean. Mar. Geol. 149, 39–54.
Puig, P., Palanques, A., 1998b. Temporal variability and composition of settling particle fluxes on the Barcelona continental margin (northwestern Mediterranean). J. Mar. Res. 56, 639–654.
R Development Core Team, 2020. R: A language and environment for statistical computing. R Foundation for Statistical Computing, Vienna, Austria.
Radabaugh, K.R., Hollander, D.J., Peebles, E.B., 2013. Seasonal $\delta^{13}C$ and $\delta^{15}N$ isoscapes of fish populations along a continental shelf trophic gradient. Cont. Shelf Res. 68, 112–122.
Ramirez-Llodra, E., Brandt, A., Danovaro, R., De Mol, B., Escobar, E., German, C., Levin, L., Arbizu, P., Menot, L., Buhl-Mortensen, P., Narayanaswamy, B.E., Smith, C. R., Tittensor, D.P., Tyler, P.A., Vanreusel, A., Vecchione, M., 2010. Deep, diverse and definitely different : unique attributes of the world's largest ecosystem. Biogeosciences 7, 2851–2899.

Rau, G.H., Teyssie, J.L., Rassoulzadegan, F., Fowler, S.W., 1990. $^{13}C/^{12}C$ and $^{15}N/^{14}N$ variations among size-fractionated marine particles - implications for their origin and trophic relationships. Mar. Ecol. Prog. Ser. 59, 33–38.

Reddin, C.J., Bothwell, J.H., O'Connor, N.E., Harrod, C., 2018. The effects of spatial scale and isoscape on consumer isotopic niche width. Funct. Ecol. 32, 904–915.

Rengstorf, A.M., Yesson, C., Brown, C., Grehan, A.J., 2013. High-resolution habitat suitability modelling can improve conservation of vulnerable marine ecosystems in the deep sea. J. Biogeogr. 40, 1702–1714.

Ribeiro Jr., P., Diggle, P., 2001. geoR: A package for geostatistical analysis. Pages 15-18 R-News.

Robert, K., Jones, D.O.B., Tyler, P.A., Van Rooij, D., Huvenne, V.A.I., 2015. Finding the hotspots within a biodiversity hotspot: fine-scale biological predictions within a submarine canyon using high-resolution acoustic mapping techniques. Marine Ecology-an Evolutionary Perspective 36, 1256–1276.

Robertson, C.M., Demopoulos, A.W.J., Bourque, J.R., Mienis, F., Duineveld, G.C.A., Lavaleye, M.S.S., Koivisto, R.K.K., Brooke, S.D., Ross, S.W., Rhode, M., Davies, A.J., 2020. Submarine canyons influence macrofaunal diversity and density patterns in the deep-sea benthos. Deep Sea Res. Part I 159, 103249.

Romero-Romero, S., Molina-Ramírez, A., Höfer, J., Duineveld, G., Rumín-Caparrós, A., Sanchez-Vidal, A., Canals, M., Acuña, J.L., 2016. Seasonal pathways of organic matter within the Avilés submarine canyon: food web implications. Deep Sea Res. Part I 117, 1–10.

Ross, S.W., Brooke, S., Quattrini, A.M., Rhode, M., Watterson, J.C., 2015. A deep-sea community, including *Lophelia pertusa*, at unusually shallow depths in the western North Atlantic Ocean off northeastern Florida. Biology Marine 1–14.

Ross, S. W., S. Brooke, E. Baird, D. K. Coykendall, A. J. Davies, A. W. J. Demopoulos, S. C. France, C. A. Kellogg, R. Mather, F. Mienis, C. Morrison, N. Prouty, B. Roark, C. M. Robertson, and S. (CSA Ocean Sciences Inc., FL). 2017. Exploration and Research of Mid-Atlantic Deepwater hard Bottom Habitats and Shipwrecks with Emphasis on Canyons and Coral Communities: Atlantic Deepwater Canyons Study. Vol I. Final Technical Rept., Vol. II: Final Appendices., U.S. Dept. of the Interior, Bureau of Ocean Energy Management, Atlantic OCS Region.

Rumolo, P., Cartes, J.E., Fanelli, E., Papiol, V., Sprovieri, M., Mirto, S., Gherardi, S., Bonanno, A., 2015. Seasonal variations in the source of sea bottom organic matter off Catalonia coasts (western Mediterranean): links with hydrography and biological response. J. Oceanogr. 71, 325–343.

Schmiedl, G., de Bovee, F., Buscail, R., Charriere, B., Hemleben, C., Medernach, L., Picon, P., 2000. Trophic control of benthic foraminiferal abundance and microhabitat in the bathyal gulf of lions, western Mediterranean Sea. Mar. Micropaleontol. 40, 167–188.

Sherwood, O.A., Jamieson, R.E., Edinger, E.N., Wareham, V.E., 2008. Stable C and N isotopic composition of cold-water corals from the Newfoundland and Labrador continental slope: examination of trophic, depth and spatial effects. Deep-Sea Research Part I-Oceanographic Research Papers 55, 1392–1402.

St John Glew, K., Graham, K.L.J., McGill, R.A.R., Trueman, C.N., 2019. Spatial models of carbon, nitrogen and sulphur stable isotope distributions (isoscapes) across a shelf sea: an INLA approach. Methods Ecol. Evol. 10, 518–531.

St John Glew, K., B. Espinasse, B. P. V. Hunt, E. A. Pakhomov, S. J. Bury, M. Pinkerton, S. D. Nodder, A. Gutierrez-Rodriguez, K. Safi, J. C. S. Brown, L. Graham, R. B. Dunbar, D. A. Mucciarone, S. Magozzi, C. Somes, and C. N. Trueman. 2021. Isoscape Models of the Southern Ocean: Predicting Spatial and Temporal Variability in Carbon and Nitrogen Isotope Compositions of Particulate Organic Matter. Global Biogeochemical Cycles **35**.

Stefanescu, C., Morales-Nin, B., Massutí, E., 1994. Fish assemblages on the slope in the Catalan Sea (western Mediterranean): influence of a submarine canyon. Journal of Marine Biological Association of UK 74, 499–512.

Thibault, M., Duprey, N., Gillikin, D.P., Thebault, J., Douillet, P., Chauvaud, L., Amice, E., Munaron, J.M., Lorrain, A., 2020. Bivalve $\delta^{15}N$ isoscapes provide a baseline for urban nitrogen footprint at the edge of a world heritage coral reef. Mar. Pollut. Bull. 152.

Thomsen, L., Gust, G., 2000. Sediment erosion thresholds and characteristics of resuspended aggregates on the western european continental margin. Deep-Sea Research Part I-Oceanographic Research Papers 47, 1881–1897.

Troina, G.C., Dehairs, F., Botta, S., Di Tullio, J.C., Elskens, M., Secchi, E.R., 2020. Zooplankton-based $\delta^{13}C$ and $\delta^{15}N$ isoscapes from the outer continental shelf and slope in the subtropical western South Atlantic. Deep-Sea Research Part I-Oceanographic Research Papers 159. https://doi.org/10.1016/j.dsr.2020.103235.

Trueman, C., St John Glew, K. 2019. Isotopic tracking of marine animal movement. Pages 137-172 Tracking animal migration with stable isotopes. New York: Elsevier.

Trueman, C.N., Johnston, G., O'Hea, B., MacKenzie, K.M., 2014. Trophic interactions of fish communities at midwater depths enhance long-term carbon storage and benthic production on continental slopes. Proceedings of the Royal Society B-Biological Sciences **281**.

Trueman, C.N., MacKenzie, K.M., St John Glew, K.S., 2017. Stable isotope-based location in a shelf sea setting: accuracy and precision are comparable to light-based location methods. Methods Ecol. Evol. 8, 232–240.

Tyler, P.A., Bronsdon, S.K., Young, C.M., Rice, A.L., 1995. Ecology and gametogenic biology of the genus umbellula (pennatulacea) in the North-Atlantic Ocean. Int. Rev. Gesamten Hydrobiol. 80, 187–199.

van den Beld, I.M.J., Guillaumont, B., Menot, L., Bayle, C., Arnaud-Haond, S., Bourillet, J.-F., 2017. Marine litter in submarine canyons of the Bay of Biscay. Deep Sea Res. Part II 145, 142–152.

Vokhshoori, N.L., Larsen, T., McCarthy, M.D., 2014. Reconstructing $\delta^{13}C$ isoscapes of phytoplankton production in a coastal upwelling system with amino acid isotope values of littoral mussels. Mar. Ecol. Prog. Ser. 504, 59–72.

Vokhshoori, N.L., McCarthy, M.D., 2014. Compound-specific $\delta^{15}N$ amino acid measurements in Littoral mussels in the California upwelling ecosystem: a new approach to generating baseline $\delta^{15}N$ isoscapes for coastal ecosystems. PLoS One 9.

Wagner, D., Luck, D.G., Toonen, R.J., 2012. The biology and ecology of black corals (Cnidaria: Anthozoa: Hexacorallia: Antipatharia). Adv. Mar. Biol. 63 (63), 67–132.

Waite, A.M., Raes, E., Beckley, L.E., Thompson, P.A., Griffin, D., Saunders, M., Sawstrom, C., O'Rorke, R., Wang, M., Landrum, J.P., Jeffs, A., 2019. Production and ecosystem structure in cold-core vs. warm-core eddies: implications for the zooplankton isoscape and rock lobster larvae. Limnol. Oceanogr. 64, 2405–2423.

Walbridge, S., Slocum, N., Pobuda, M., Wright, D.J., 2018. Benthic terrain modeler (BTM) 3.0, tools for understanding and classifying the benthic environment. Geosci. J.**8**:94.

West, J.B., Sobek, A., Ehleringer, J.R., 2008. A simplified GIS approach to modeling global leaf water isoscapes. PLoS One 3.

Wilson, M.F.J., Oâ€™Connell, B., Brown, C., Guinan, J.C., Grehan, A.J., 2007. Multiscale terrain analysis of multibeam bathymetry data for habitat mapping on the continental slope. Mar. Geod. 30, 3–35.

Woolley, S.N.C., Tittensor, D.P., Dunstan, P.K., Guillera-Arroita, G., Lahoz-Monfort, J.J., Wintle, B.A., Worm, B., O'Hara, T.D., 2016. Deep-sea diversity patterns are shaped by energy availability. Nature 533, 393–396.

Young, J.W., Blaber, S.J.M., 1986. Feeding ecology of 3 species of midwater fishes associated with the continental-slope of eastern Tasmania, Australia. Mar. Biol. 93, 147–156.

Zar, J.H., 1999. Biostatistical analysis, 4th edition. Prentice Hall, Upper Saddle River, NJ.